The Report Committee for Ahra Lee
Certifies that this is the approved version of the following report:

A POLYMER HYDROLYSIS MODEL AND ITS APPLICATION IN

CHEMICAL EOR PROCESS SIMULATION

APPROVED BY

SUPERVISING COMMITTEE:

Supervisor:

Gary A. Pope

Co-Supervisor:

Mojdeh Delshad

A POLYMER HYDROLYSIS MODEL AND ITS APPLICATION IN CHEMICAL EOR PROCESS SIMULATION

by

Ahra Lee, B.S., M.S.

Report

Presented to the Faculty of the Graduate School of

The University of Texas at Austin

in Partial Fulfillment

of the Requirements

for the Degree of

Master of Science in Engineering

The University of Texas at Austin

December 2010

Dedication

To my families in the United States and Korea

Acknowledgements

Abstract

A POLYMER HYDROLYSIS MODEL AND ITS APPLICATION IN CHEMICAL EOR PROCESS SIMULATION

Ahra Lee, M.S.E.

The University of Texas at Austin, 2010

Supervisor: Gary A. Pope

Co-supervisor: Mojdeh Delshad

Polymer flooding is a commercial enhanced oil recovery (EOR) method used to increase the sweep efficiency of water floods. Hydrolyzed polyacrylamide (HPAM), a synthetic commercial polymer, is widely used in commercial polymer floods and it is also used for mobility control of chemical floods using surfactants such as surfactant-polymer flooding and alkaline-surfactant-polymer flooding. The increase in the degree of hydrolysis of HPAM at elevated temperature or pH with time affects the polymer solution viscosity and its adsorption on rock surfaces.

A polymer hydrolysis model based on published laboratory data was implemented in UTCHEM, a chemical EOR simulator, in order to assess the effect of hydrolysis on

reservoir performance. Both 1D and 3D simulations were performed to validate the implementation of the model.

The simulation results are consistent with the laboratory observations that show an increase in polymer solution viscosity as hydrolysis progresses. The numerical results indicate that hydrolysis occurs very rapidly and impacts the near wellbore region polymer injectivity.

Table of Contents

List of Tables

List of Figures

Chapter 1: INTRODUCTION

After primary depletion of an oil reservoir, water is often injected to increase the reservoir pressure and oil production rate. This secondary recovery method, however, still leaves behind a substantial amount of oil due to both residual oil saturation in the pores of the rock and incomplete sweep in heterogeneous reservoirs. Since the 1960's, adding water-soluble polymer has been used to increase the water viscosity (lower the mobility ratio) to improve the reservoir sweep efficiency, and consequently to increase oil recovery. Polymer flood is not only economically acceptable, but promising for helping to meet the high oil and gas production demands.

Many researchers have focused on the stability of EOR polymers, especially partially hydrolyzed polyacrylamides (HPAM), under reservoir conditions (Muller, 1981; Kulicke and Horl, 1985; Kheradmand, 1987; Moradi-Araghi and Doe, 1987; Sorbie, 1991). More recently, Levitt (2009, 2010) did experimental research using polyacrylamide polymers under various hostile conditions.

One of the most important characteristic of HPAM polymer is hydrolysis. Widely used polyacrylamides hydrolyze as time passes, and its viscosity increases. The negative charges along its chain, as a result of hydrolysis, repulse each other in the chain and the chain extends, thereby increasing the viscosity. Therefore, initially unhydrolyzed polymer has the lowest viscosity. Lakatos et al. (1979) observed that unhydrolyzed polyacrylamide had extremely high values of adsorption. Therefore, the unhydrolyzed polymer with lower viscosity compared to hydrolyzed polymer has a more favorable injectivity but at the expense of higher adsorption. Most available polymers are HPAM where their injection pressure is relatively higher with a lower adsorption tendency compared to the unhydrolyzed molecule. The hydrolysis of polymers has an important

role in terms of aqueous phase viscosity and injectivity in chemical EOR processes such as polymer, surfactant-polymer (SP), and alkaline-surfactant-polymer (ASP) flooding. It has become imperative to understand and fully characterize the hydrolysis of HPAM polymers.

The objective of this study was to develop a polymer hydrolysis model and implement it into an existing chemical flooding simulator called UTCHEM. After the implementation of this new feature, it was tested to evaluate the effect of polymer hydrolysis on the performance of the polymer in reservoirs.

This report has been divided into five chapters including the current chapter. In Chapter 2, a review of early work concerning polymer on EOR and the hydrolysis is discussed. A review of UTCHEM simulator is also presented in this chapter. Chapter 3 introduces the proposed polymer hydrolysis model and its implementation into UTCHEM. Chapter 4 deals with the simulation results using enhanced simulator for both simple 1D cases and 3-D pilot cases. Finally, the conclusions of this study are presented in Chapter 5.

Chapter 2: BACKGROUND

2.1 A LITERATURE REVIEW OF POLYMER

2.1.1 Polymers on Enhanced Oil Recovery

After primary depletion of the reservoir pressure, in order to displace oil, mainly suggested way to maintain reservoir pressure is injecting water, which is called waterflooding. This secondary oil recovery often causes flow channeling and leaves substantial bypassed oil in heterogeneous reservoirs. Enhanced oil recovery (EOR) processes such as polymer flooding or surfactant-polymer flooding use polymer to reduce fluid mobility to improve the sweep efficiency of the reservoir, i.e., to increase the volume of the reservoir contacted at any given time (Lake, 1989; Sorbie, 1991).

Commercically available polymers have been applied in to improve water flood oil recovery since the 1060s. Putz et al. (1988) and Koning et al. (1988) report successful polymer floods. The polymer flood of the Daqing oil field is one of the largest and most successful polymer floods (Wang et al., 2001)

2.1.2 Polymer Hydrolysis

Technically, hydrolysis is defined as a chemical reaction in the presence of water. Polyacrylamide (PAM), which is a homopolymer of acrylamide, hydrolyzes at a certain amide site to an anionically charged carboxyl group. The increased charge density along the HPAM backbone extends the polymer coil and increases solution viscosity. Hydrolysis of PAM and its structure are presented in Figure 2.1. These partially hydrolyzed polyacrylamides (HPAM) are commercially available synthetic polymers and they are by far the most widely used polymers for EOR.

3

Polymer hydrolysis is mostly affected by pH and temperature and has been the subject of many papers. Lakatos et al. (1979) studied the factors influencing polyacrylamide adsorption in porous media such as average molecular mass, degree of hydrolysis, and polymer concentration. Muller (1981) reported thermal stability of high-molecular-weight polyacrylamide aqueous solutions at various initial pH values. Moradi-Araghi and Doe (1987) performed an extensive investigation on hydrolysis and precipitation of PAM without using a buffer. They found that hydrolysis continues until the complete hydrolysis of amide sites. The hydrolysis is faster at higher temperature. They also observed the PAM precipitation as a function of the calcium concentration. Kulicke and Horl (1985) characterized various molecules of polyacrylamide polymer solution by measuring properties such as intrinsic viscosity. Ryles (1988) and Seright and Mozley (2009) studied the chemical stability of HPAM at elevated temperature in the absence of dissolved oxygen.

More recently, Choi (2008) studied the HPAM viscosity dependence on pH at different degrees of hydrolysis. He observed that the pH sensitivity is more pronounced as the degree of hydrolysis increases. Levitt et al. (2010) proposed using a HPAM with a low degree of hydrolysis to benefit from higher injectivity due to its lower initial viscosity. They pointed out that the aqueous phase viscosity will increases once the polymer hydrolyzes in the reservoir.

2.2 A REVIEW OF UTCHEM SIMULATOR

2.2.1 General Description of the Simulator

UTCHEM, the University of Texas Chemical Flooding Simulator, is a three-dimensional, multicomponent chemical flooding simulator developed by The University

of Texas at Austin (UTCHEM Technical Documentation, 2000). The simulator takes into account aqueous species such as water, electrolytes (anions and cations), chemical species such as surfactant, polymer, tracer, and oleic species such as crude oil. These components may form up to three liquid phases – aqueous, oleic, and microemulsion-depending on the amount and effective salinity of the phase environment. UTCHEM can model a variety of oil recovery applications such as

waterflooding

polymer flooding

profile control using polymer gel or foam

surfactant flooding

alkaline flooding

alkaline-surfactant-polymer flooding

alkaline-surfactant-gas flooding

microbial EOR

2.2.2 Modeling of Reacting Tracer

UTCHEM models any number of tracers, which can be water tracer, oil tracer, partitioning oil/water tracer, gas tracer, partitioning gas/oil tracer, and up to two reacting tracers. Only water/oil tracers can be considered as reacting tracers and they are accompanied by reacting tracer and its product.

The following assumptions have been made in developing the reacting tracer model in UTCHEM:

1. Tracers do not occupy volume

2. Tracers have no effect on the physical properties

The overall tracer concentrations are computed from the species conservation equations which include a reaction term for the reacting tracer.

The reaction of a reacting tracer such as acetate is shown below:

Hydrolysis of an ester to form an alcohol is assumed to be irreversible and of first order, which means one mole of acetate generates one mole of product alcohol.

$$1CH_2COO[C_nH_{2n+1}]+1H_2O \rightarrow 1C_nH_{2n+1}[OH]+1C_2H_4O_2 \tag{2-1}$$
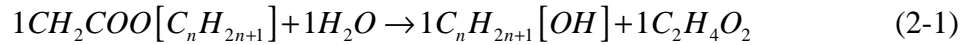
The reaction is modeled as

$$\frac{\partial C_{10}}{\partial t} = -K_hC_{10} \tag{2-2}$$

$$\frac{\partial C_{11}}{\partial t} = K_hC_{10} \tag{2-3}$$

Where K_h is the reaction rate constant in day^{-1} and C_{10} and C_{11} are concentrations of 10th and 11th component, which are reacting tracer and its product, respectively.

2.2.3 Modeling of Polymer

2.2.3.1 Polymer Solution Viscosity at Zero Shear Rate

The polymer solution viscosity at zero shear rate is calculated as a function of polymer and electrolyte concentrations. The Flory–Huggins equation (Flory, 1953) was modified to account for variation in salinity as:

$$\mu_p = \mu_w \left[1+\left(A_{p1}c_{4\ell} + A_{p2}c_{4\ell}^2 + A_{p3}c_{4\ell}^3\right)C_{SEP}^{Sp}\right] \tag{2-4}$$

where $C_{4\ell}$ is the polymer concentration in the water or microemulsion phase, μ_w is the water viscosity. A_{p1}, A_{p2}, and A_{p3} are empirical constants for a given polymer and are

determined from experimental data. C_{SEP} is the effective salinity, defined for use in polymer property calculations:

$$C_{SEP} = \frac{C_5 + (\beta_p - 1)C_6}{C_1} \tag{2-5}$$

β_p is a parameter used to determine the effects of divalent cations on the effective salinity for polymer. Subscripts, which are specie index, 1, 4, 5, and 6 refer to water, polymer, chloride, and calcium, respectively. The second subscript ℓ is the phase index, which is either aqueous phase or microemulsion phase. Sp is an input parameter to determine polymer viscosity as a function of salinity. Plotting $\frac{\mu_0 - \mu_w}{\mu_w}$ vs. C_{SEP}, which is assumed to be a straight line on a log-log plot, gives Sp. This slope is negative for hydrolyzed polyacrylamides.

2.2.3.2 Polymer Adsorption

The retention of polymer molecules in permeable media is due to not only adsorption onto solid surfaces but also trapping within small pores. The polymer retention slows down the polymer velocity and depletes the polymer slug. Polymer adsorption modeled in UTCHEM uses a Langmuir-type isotherm which takes into account the salinity, permeability, and polymer concentration. The adsorbed concentration of polymer is given by

$$\hat{C}_4 = \min\left(\tilde{C}_4, \frac{a_4\left(\tilde{C}_4 - \hat{C}_4\right)}{1 + b_4\left(\tilde{C}_4 - \hat{C}_4\right)} \right) \tag{2-6}$$

The concentrations are normalized by the water concentration in the adsorption calculations. The minimum is taken to guarantee that the adsorption is no greater than the total polymer concentration. The parameter a_4 is defined as

$$a_4 = \left(a_{41} + a_{42}C_{SEP}\right)\left(\frac{k_{ref}}{k}\right)^{0.5} \tag{2-7}$$

where k_{ref} is the reference permeability at which the input adsorption parameters are defined, a_{41} and a_{42} are the input parameters found by matching laboratory polymer adsorption data, and C_{SEP} is the effective salinity for polymer. b_4 controls the curvature of the isotherm and a_4/b_4 indicates the plateau value of adsorbed polymer. Adsorption increases linearly with effective salinity for polymer and decreases as the permeability increases.
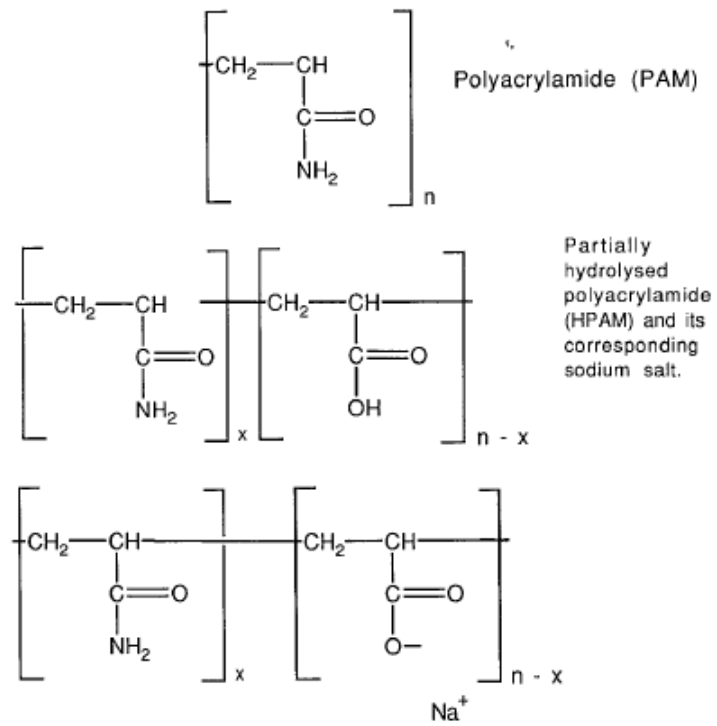
Figure 2.1: The primary chain structure of polyacrylamide (PAM) and partially
hydrolyzed polyacrylamide (HPAM) (Sorbie, 1991)

Chapter 3: POLYMER HYDROLYSIS MODEL

This chapter describes the proposed polymer hydrolysis model and its implementation in UTCHEM.

3.1 MODEL DESCRIPTION

Models developed to calculate polymer hydrolysis and its viscosity effect are presented here.

3.1.1 Relationship between the Degree of Hydrolysis and Time

In Chapter 2, polymer hydrolysis was discussed. As shown in Figure 2.1., HPAM has amide groups and carboxylic groups. Consider a polymer molecule which initially has N amide side groups. As some of the amide groups are replaced with carboxylic group according to the hydrolysis, the degree of hydrolysis, τ in fraction, increases. If the rate of hydrolysis is proportional to the number of the amide groups available, then

$$\frac{d(N\tau)}{dt} = kN(1-\tau) \qquad (3\text{-}1)$$

where k is the reaction rate constant. However, because of the electrostatic charge of the carboxylic group, which is anionic, the replacement of the amide groups in the neighborhood of the carboxylic groups will be different. Therefore, we can approximate

$$\frac{d(N\tau)}{dt} = kN(1-\tau)^m \qquad (3\text{-}2)$$

where m is the exponent of the reaction with a value great than one. The above equation implies that as the hydrolysis progresses, the rate will decrease as shown in Figure 3.1. Initially, the rate is similar to the case with $m = 1$ case, but it decreases much faster as hydrolysis progresses. By solving Equation (3-2):

$$\frac{d\tau}{dt} = k(1-\tau)^m \tag{3-3}$$

$$(1-\tau)^{-m} d\tau = kdt \tag{3-4}$$

$$-\frac{(1-\tau)^{1-m}}{1-m} = kt + C \tag{3-5}$$

The initial condition is that $\tau = 0$ when $t = 0$. Therefore,

$$C = -\frac{1}{1-m} \tag{3-6}$$

$$(1-\tau)^{1-m} = (m-1)kt + 1 \tag{3-7}$$

$$(1-\tau) = \left[(m-1)kt + 1\right]^{\frac{1}{1-m}} \tag{3-8}$$

$$\therefore \tau = 1 - \left[(m-1)kt + 1\right]^{\frac{1}{1-m}} \tag{3-9}$$

Based on the experimental data at a fixed temperature provided by Moradi-Araghi and Doe (1987), the best-fit values of m and k were obtained by fitting the data with Equation (3-9). The value of m is between 1 and 2 regardless of the temperature. However, k increases as temperature increases. We can assume a value of 1.6 for m based on the best-fit to the data. The dependency of k on temperature is modeled using

the Arrhenius equation $k = k_0 e^{-\Delta E / RT}$. The Arrhenius equation fit to the data is expressed as follows:

$$\ln k = -\frac{\Delta E}{R}\frac{1}{T} + \ln k_0 \tag{3-10}$$

$$\ln k = -10981\frac{1}{T} + 27.149 \tag{3-11}$$

$$\therefore \ln k = -\frac{91.3}{R}\frac{1}{T} + 27.149 \tag{3-12}$$

where, $\Delta E = 91.3 KJ/mol$.

In summary, the degree of hydrolysis as a function of time is modeled as a kinetic reaction model:

$$\left[\frac{d\tau}{dt}\right]_H = k(1-\tau)^{1.6} \tag{3-13}$$

where, the effect of temperature on the reaction rate constant is calculated from $\ln k = -\frac{91.3}{R}\frac{1}{T} + 27.149$.

3.1.2 Relationship between the Ratio of the Intrinsic Viscosity and the Degree of Hydrolysis

The polymer viscosity data as a function of the degree of hydrolysis are fairly scarce. Kulicke and Horl (1985) characterized various copolymer compositions of polyacrylamide-co-acrylates. They reported the ratios of the intrinsic viscosities of polyacrylamide (PAM) /sodium acrylate, which is hydrolyzed PAM, to the value of the initial PAM. The intrinsic viscosity, designated as $[\eta]$, is independent of polymer

12

concentration but dependent on the size of molecule in solution, and is a more fundamental quantity of polymer solution viscosity. The intrinsic viscosity is the limit of the reduced viscosity or inherent viscosity as the solution concentration of polymer tends to zero (Sorbie, 1991):

$$[\eta] = \mathop{Lim}_{C_P \to 0} \eta_R = \mathop{Lim}_{C_P \to 0} \frac{\eta - \eta_s}{C_P \eta_s} \tag{3-14}$$

$$[\eta] = \mathop{Lim}_{C_P \to 0} \eta_I = \mathop{Lim}_{C_P \to 0} \frac{\ln \eta_r}{C_P} \tag{3-15}$$

η is the polymer solution viscosity, η_R is the reduced viscosity, η_s is the solvent viscosity, C_p is the polymer concentration, η_I is the inherent viscosity, and η_r is the relative viscosity.

Based on Kulicke and Horl's data (Figure 3.3), the relationship between the intrinsic viscosity of hydrolyzed PAM and the degree of hydrolysis can be obtained empirically:

$$\Lambda_p = \frac{1}{1 - 1.4335\tau} \tag{3-16}$$

where, Λ_p is the ratio of the intrinsic viscosity of PAM and HPAM as $[\eta]/[\eta]_{PAM}$.

3.1.3 Effect of Polymer Hydrolysis on Adsorption

Lakatos et al. (1979) reported various factors influencing polyacrylamide adsorption. They found that amount adsorbed decreased slightly with increasing average molecular mass but decreased more sharply as the degree of hydrolysis increased. Based

13

on this experimental data, adsorption of polyacrylamide as a function of the degree of hydrolysis is modeled as shown in Figure 3.4:

$$\hat{C}_4 = \hat{C}_{40} \exp\left(K_{4a}\tau'\right)$$
(3-17)

τ' is the degree of hydrolysis in percent, $\hat{C}_{40}$ is polymer adsorption for unhydrolyzed polymer, and K_{4a} is an empirical constant for polymer adsorption as a function of polymer hydrolysis. The value for K_{4a} found to be (-0.0355) using the data of Lakatos et al. (1979). It is noted that the meaured data gives an extremely high adsorption of hydrolyzed polyacrylamide (Fig.3.4) compared with more recently observed experimental data in the range of 20 - 40 µg/g rock. We speculate that the high adsorption is because of improper polymer filtration prior to the coreflood experiment.

3.2 HYDROLYSIS MODEL APPLICATION INTO UTCHEM

Numerous modifications were made in UTCHEM source code to implement the polymer hydrolysis model.

3.2.1 Degree of Polymer Hydrolysis using Reacting Tracer Option

Lange and Huh (1994) suggested a novel way to model the thermal decomposition of biopolymer using a tracer. The average molecular weight of thermally decomposed polymer is calculated using tracer reaction with thermal decomposition rate, and this average molecular weight could be directly related to viscosity in the low-shear-rate limit at any concentration. For simulation of polymer hydrolysis, the reacting tracer (the 10th component) already modeled in UTCHEM can be used as if the degree of

14

hydrolysis is the concentration of the reacting tracer. The reacting tracer gradually decreases according to an input reaction rate as shown in Equation (2-2). Similarly, unhydrolyzed fraction of polymer also decreases according to the reaction rate as time passes. Therefore, for the polymer hydrolysis model, Equation (1-13) can be modified as:

$$\frac{d(1-\tau)}{dt} = -k(1-\tau)^{1.6} \quad \Leftrightarrow \quad \frac{dC_{10}}{dt} = -kC_{10}^{1.6} \tag{3-18}$$

It is noted that $\tau = 1 - C_{10}$ is equal to $\tau = 1 - C_{10}$. For example, initial reacting tracer concentration equal to 0.7 means that a polymer with 30% degree of hydrolysis is injected. The reacting tracer is continuously injected to obtain the degree of hydrolysis of polymer in the reservoir as a function of time. The calculated degree of hydrolysis is then used for polymer viscosity calculations.

For practical applications, a maximum value for the degree of hydrolysis is assumed. Therefore;

$$\tau = \left[\text{max. constraint for degree of hydrolysis}\right] - C_{10} \tag{3-19}$$

3.2.2 Hydrolysis-Dependent Polymer Viscosity Model

Polymer viscosity is modeled as a function of polymer concentration, salinity and shear rate. UTCHEM simulator requires input parameters for each of these models. From the Equation (3-14), intrinsic viscosity can be redefined with:

$$[\eta] = \underset{C_P \to 0}{Lim} \frac{\eta - \eta_s}{C_P \eta_s} = \underset{C_P \to 0}{Lim} \frac{\eta_r - 1}{C_p} \tag{3-20}$$

where $\eta_r = \frac{\eta}{\eta_s}$. Using Equation (2-4) the relative viscosity in UTCHEM is defined:

$$\eta_r = \frac{\mu_o}{\mu_w} = 1 + \left(A_{p1}c_{4\ell} + A_{p2}c_{4\ell}{}^2 + A_{p3}c_{4\ell}{}^3 \right) C_{SEP}^{Sp} \tag{3-21}$$

Therefore, the intrinsic viscosity calculation in UTCHEM is:

$$[\eta] = \mathop{Lim}_{C_P \to 0} \frac{\left[1 + \left(A_{p1}c_{4\ell} + A_{p2}c_{4\ell}{}^2 + A_{p3}c_{4\ell}{}^3 \right) C_{SEP}^{Sp} \right] - 1}{C_p} \tag{3-22}$$

$$[\eta] = \mathop{Lim}_{C_P \to 0} \left(A_{p1} + A_{p2}c_{4\ell} + A_{p3}c_{4\ell}{}^2 \right) C_{SEP}^{Sp} \tag{3-23}$$

$$[\eta] = A_{p1} C_{SEP}^{Sp} \tag{3-24}$$

The empirical constant A_{p1} has a linear relationship with the intrinsic viscosity (Equation 3-24). The intrinsic viscosity modeled in UTCHEM is, precisely, the intrinsic viscosity of PAM. Combining this relationship with Kulicke and Horl's result shows:

$$[\eta]_{PAM} = A_{p1} C_{SEP}^{Sp} \tag{3-25}$$

$$[\eta] = A_{p1}{}^{new} C_{SEP}^{Sp} \tag{3-26}$$

$$[\eta] = \Lambda_P [\eta]_{PAM} = \Lambda_P A_{p1} C_{SEP}^{Sp} \tag{3-27}$$

$$\therefore A_{p1}{}^{new} = \Lambda_p \times A_{p1} \tag{3-28}$$

Therefore, the effect of polymer hydrolysis on solution viscosity is modeled by multiplying A_{p1} by Λ_p given in Eq. 3-17.

3.2.3 Hydrolysis Dependent Polymer Adsorption

The adsorbed concentration of polymer is calculated in UTCHEM using Equation (2-6). UTCHEM calculates polymer concentration and adsorbed polymer concentration once at every gridblock at each time step. Polymer adsorption is a function of degree of hydrolysis, therefore polymer concentration and its adsorption should be calculated as the degree of hydrolysis changes. Once polymer adsorption at a given degree of hydrolysis is determined, Equation (3-18) will be used to adjust the adsorption parameter (a_{41}) as a function of degree of hydrolysis.
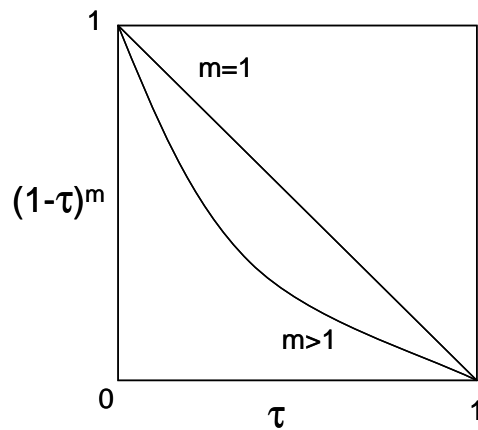
Figure 3.1: Relationship between amide groups and carboxylic groups in a polymer
molecule.
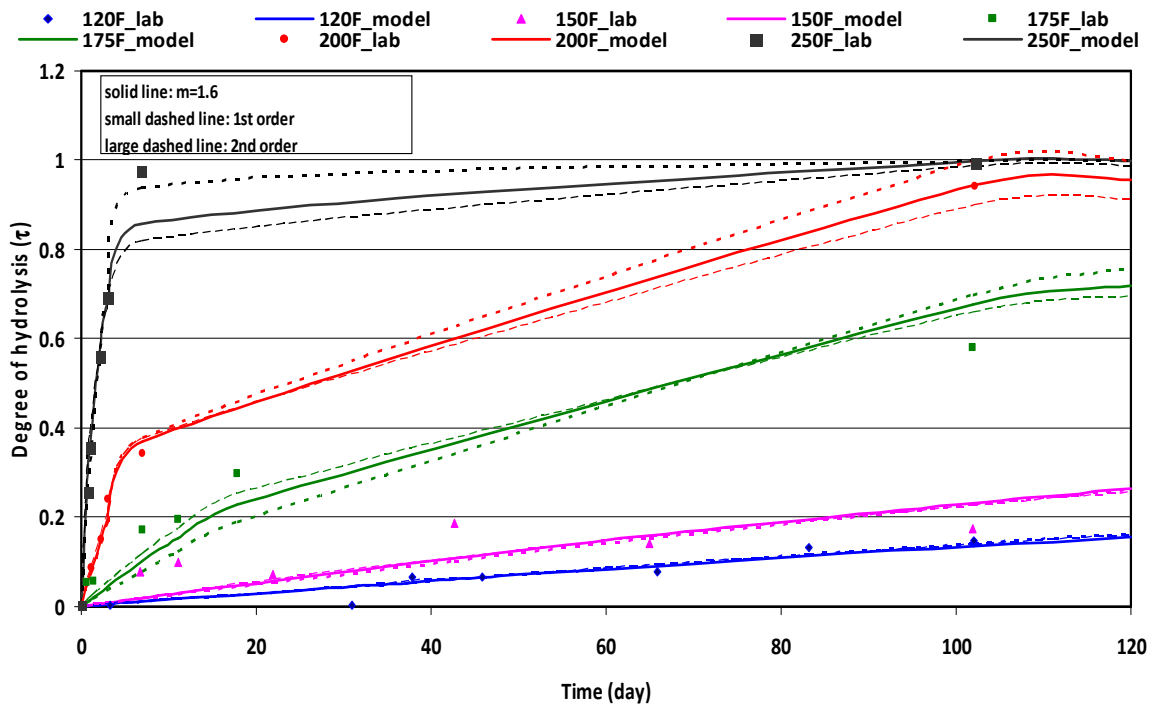
Figure 3.2: Comparison of calculated and measured degree of hydrolysis as a function of
time at fixed temperatures (data from Moradi-Araghi and Doe, 1987)

18
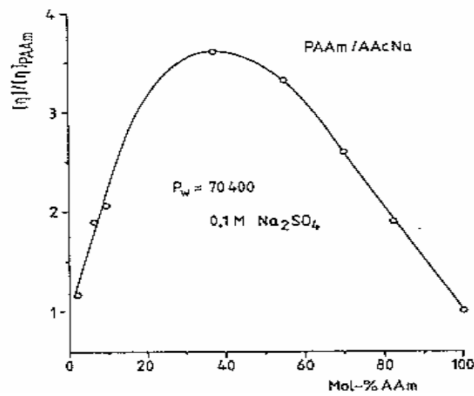
Figure 3.3: Ratio of the intrinsic viscosities of polyacrylamide (PAM) /sodium acrylate, which is hydrolyzed PAM, to the value of the initial PAM (Kulicke and Horl, 1985)
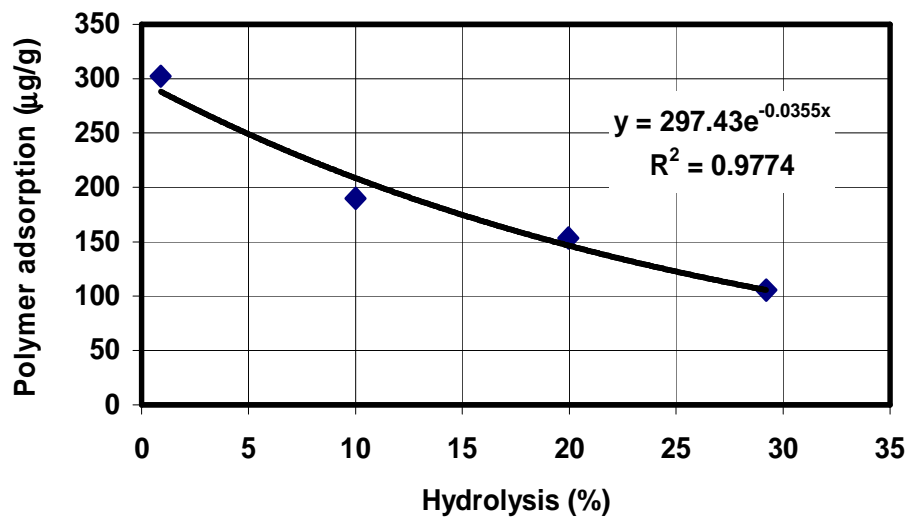
Figure 3.4: HPAM adsorbed concentration on silica sand as a function of degree of hydrolysis (data from Lakatos et al., 1979)

19

Chapter 4: SIMULATION RESULTS

Both 1D core flood and 3D field simulations were set up to test and validate the polymer hydrolysis model and its implementation in UTCHEM. In this chapter, specific simulation results are presented. The effect of polymer hydrolysis as a function of time was first simulated on the core flood scale and then on the field scale.

4.1 CORE FLOOD SIMULATION RESULTS

One-dimensional coreflood simulations were first performed. In order to allow for sufficient time for hydrolysis to occur, longer cores were simulated. The input parameters for this single-phase, 1D displacement are shown in Table 4.1. Table 4.2 gives the summary of the simulated cases. The reservoir temperature condition simulated provides favorable condition for polymer hydrolysis in order to visualize the effect of hydrolysis on viscosity.

Polymer hydrolysis effect on polymer viscosity

After a 0.7 PV of polymer slug is injected, water is injected to push the polymer and oil towards the producer. Injected polymer concentration is 1200 ppm. In this simulation, the effect of polymer hydrolysis on adsorption is not modeled.

Figure 4.1(a) and (b) show the polymer concentration and viscosity profiles at 1.0 PV injected. When the polymer hydrolysis model is considered, polymer viscosity changes as polymer propagates. Hydrolysis increased as a function of time and viscosity also increased as a function of rate of hydrolysis, so viscosity increase in the core as a function of time in the core is demonstrated.

Polymer adsorption effect on polymer viscosity

In order to validate the polymer adsorption effect on polymer viscosity, 30% initially hydrolyzed polyacrylamide is injected with and without polymer adsorption. Figure 4.2(a) has no adsorption effect on the calculation of polymer concentration and its viscosity, while Figure 4.2(b) has adsorption, which is 102.53 mg/g rock based on paper research (Lakatos et al., 1979), so that the polymer concentration and its viscosity are affected.

Polymer hydrolysis and adsorption effects on polymer viscosity

Using the polymer hydrolysis model in UTCHEM with and without adsorption, initially unhydrolyzed polymer is injected. The results are shown in Figure 4.3(a) and Figure 4.3(b). The adsorption value used in this simulation comparison is also derived from Lakatos et al. (1979), which is 297.43 mg/g rock. The viscosity increase starts to appear after 7 PV because of the high value of adsorption, and while polymer exists there is an increase in viscosity.

4.2 FIELD CASE SIMULATION RESULTS

Simulation area is extended to the field-scale to study polymer hydrolysis effect on oil recovery, reservoir pressure, aqueous phase viscosity, and injected polymer mass on real field scale.

4.2.1 Pressure Constrained Polymer Injection Case

Pressure constrained injection of polymer flooding was first performed to explore the oil recovery and injected polymer mass difference with and without polymer

hydrolysis. For different values of initial water saturation, injected polymer concentration, and oil viscosity results are shown and compared.

Field descriptions and UTCHEM input parameters

This field-scale simulation model is a quarter of five-spot reservoir. Originally surfactant-polymer flooding with a constant-rate injection is modified into polymer flooding with constant-pressure injection to validate and compare the effect of polymer hydrolysis model. Injection and production wells are pressure constrained. Specific reservoir properties and injected polymer properties are summarized in Table 4.3. The effect of the degree of hydrolysis on adsorption was not modeled in this example. The reservoir temperature is 200°F. Simulated run cases are summarized in Table 4.4.

Simulation results

The cumulative oil recovery and injected polymer mass per barrel of oil produced are plotted as a function of time and PV injected for all simulation cases. All simulation results are summarized and plotted in Figure 4.4(a) to Figure 4.6(d). At different initial water saturation (from Figures 4.4(a) to (d)), cumulative oil recovery for lower water saturation case shows the best result as the way it is and there is not much difference between with and without polymer hydrolysis effects. At different initial polymer concentration injected (from Figure 4.5(a) to (d)), cumulative oil recovery is collapsed in one propagation as a function of PV injected, while cumulative oil recovery as a function of time is not. The amount of injected polymer per barrel of oil produced shows less value with polymer hydrolysis model applied on the simulation than without polymer hydrolysis. At different initial oil viscosity (from Figures 4.6(a) to (d)), beneficial effect

on polymer hydrolysis is observed in cumulative oil recovery and injected polymer amount per barrel of oil produced.

4.2.2 Injecting Flow Rate Constrained Polymer Flooding Pilot Case

The adsorption effect as a function of the degree of hydrolysis is validated using injecting flow rate constrained polymer flooding on another field scale simulation. As shown in Figure 3.4, a higher degree of hydrolysis has lower amount of polymer adsorption even with the same polymer. Therefore, without polymer hydrolysis consideration injecting initially 30% hydrolyzed polymer, with polymer hydrolysis effect coupled with adsorption injecting initially 30% hydrolyzed polymer, and with polymer hydrolysis effect coupled with adsorption injecting unhydrolyzed polymer are simulated and compared (Table 4.6).

Field descriptions and UTCHEM input parameters

The reservoir model is an inverted five-spot pattern of 200 m in the x direction (23 grid blocks), 200 m in the y direction (23 grid blocks), and 20 m in the z direction (7 grid blocks) with one injection well and four production wells. Specific reservoir properties, injected polymer properties, and injecting schedule are summarized in Table 4.5.

Initially 30% hydrolyzed polymer has an 18 µg/g rock adsorption at a polymer concentration of 1000 ppm, as shown in Table 4.5. This value can be used to calculate unhydrolyzed polymer adsorption using Equation (3-17), which is 52.2 µg/g rock. Therefore, different values of adsorption parameter for polymer were used for simulating the cases.

23

Simulation results

Consumption of polymer due to the adsorption on the rock surface cannot be neglected on polymer concentration propagation, and affects prohibitively high to the results. Viscosity comparisons with and without the polymer hydrolysis effect at different time steps are shown in Table 4.7. After water preflush, the polymer penetrated area from the injector with unhydrolyzed polymer injection with hydrolysis consideration (case #3) is less than with 30% hydrolyzed polymer injection without polymer hydrolysis consideration (case #1). This is caused by high polymer adsorption of unhydrolyzed polymer than initially 30% hydrolyzed polymer (Figure 4.7) as previously mentioned (Lakatos et al., 1979). As time passes, on the other hand, viscosity increases more in case #3 than case #1, which is caused by the hydrolysis effect on viscosity as a function of time in the reservoir. Cumulative oil recovery, average reservoir pressure, and reservoir pressure near the wellbore for each case is presented in Figure 4.8, 4.9, and 4.10, respectively.

Table 4.1: Summary of input parameters of extended 1D core flood

Reservoir Properties	
Dimensions of the core	8.8 ft x 0.11 ft x 0.11 ft
Number of grid blocks in the x, y and z directions	80 x 1 x 1
Gridblock sizes in the x, y, and z directions	0.11 ft x 0.11 ft x 0.11 ft
Porosity	0.2
Permeability	250 md
Initial pressure	14.5 psi
Residual water saturation	0.3
Water viscosity	1 cp
Brine salinity assumed all anions	0.0039 meq/ml
Divalent cation concentration of brine	0.00335 meq/ml
Longitudinal dispersivity	NONE
Transverse dispersivity	NONE
Reservoir temperature	
Parameters Related to the Polymer Properties	
Polymer viscosity parameter, A_{p1}	10 wt%$^{-1}$
Polymer viscosity parameter, A_{p2}	zero
Polymer viscosity parameter, A_{p3}	zero
Effective salinity parameter, β	20
Minimum salinity for polymer viscosity calculations, C_{SE1}	0.01 meq/ml
Slope of viscosity versus salinity on a log-log plot, S_p	-0.6
Coefficient used in shear rate equation, $\dot{\gamma}_c$	zero
Shear rate at which polymer viscosity is one half polymer viscosity at zero shear rate, $\dot{\gamma}_{1/2}$	56.10 s^{-1}
Exponent for calculating shear rate dependence of polymer viscosity, P_α	1.643
Parameter for calculating the permeability reduction, b_{rk}	100 ft^3/wt%
Parameter for calculating the permeability reduction, C_{rk}	0.0186 $\sqrt{darcy}/\sqrt[3]{100g/g}$
Polymer solution adsorption parameter, a_{41}	zero
Polymer solution adsorption parameter, a_{42}	zero
Polymer solution adsorption parameter, b_4	100 ft^3/wt%

Table 4.2: Summarized run cases of extended 1D core flood

No	Case description
1	30% hydrolyzed polymer injected without polymer adsorption and polymer hydrolysis
2	30% hydrolyzed polymer injected with polymer adsorption without polymer hydrolysis
3	Unhydrolyzed polymer injected without polymer adsorption with polymer hydrolysis
4	Unhydrolyzed polymer injected with polymer adsorption and polymer hydrolysis

Table 4.3: Summary of input parameters of pressure constrained field case

Reservoir Properties	
Dimensions of the quarter five-spot	250 ft x 250 ft x 10 ft
Number of gridblocks in the x, y and z directions	11 x 11 x 2
Grid block sizes in the x, y, and z directions	22.727 ft x 22.727 ft x 5 ft
Porosity	0.2
X direction permeability	500 md, 100 md
Y direction permeability	500 md, 100 md
Z direction permeability	50 md
Depth of reservoir	3150 ft
Initial reservoir pressure	1363.95 psi
Residual water saturation	0.37
Residual oil saturation	0.35
Endpoint relative permeability of water	0.11
Endpoint relative permeability of oil	0.95
Relative permeability exponent for the water phase	1.0
Relative permeability exponent for the oil phase	2.16
Water viscosity	0.86 cp
Oil viscosity	4 cp
Capillary pressure parameter, cpc	$9.0 \ \text{psi} \ \sqrt{\text{darcy}}$
Capillary pressure exponent, npc	2.0
Endpoint water-oil mobility ratio	0.539
Brine salinity assumed all anions	0.327 meq/ml
Divalent cation concentration of brine	0.001 meq/ml
Longitudinal dispersivity	12 ft
Transverse dispersivity	0.4 ft

Table 4.3: Summary of input parameters of pressure constrained field case (Continued)

Wellbore radius	0.5 ft
Injection wells skin	0
Production wells skin	0
Injection pressure	1540 psi
Production pressure	1363.95 psi
Parameters Related to the Polymer Properties	
Polymer viscosity parameter, $Ap1$	81 wt%$^{-1}$
Polymer viscosity parameter, $Ap2$	2700 wt%$^{-2}$
Polymer viscosity parameter, $Ap3$	2500
Effective salinity parameter, β	10
Minimum salinity for polymer viscosity calculations, CSE1	0.01 meq/ml
Slope of viscosity versus salinity on a log-log plot, Sp	0.17
Coefficient used in shear rate equation, $\dot{\gamma}c$	20 $\mathrm{day}\sqrt{\mathrm{darcy}}/(\mathrm{ft\ s})$
Shear rate at which polymer viscosity is one half polymer viscosity at zero shear rate, $\dot{\gamma}1/2$	10 s^{-1}
Exponent for calculating shear rate dependence of polymer viscosity, $P\alpha$	1.8
Ratio of apparent porosity for polymer to actual porosity Parameter for calculating the permeability reduction, brk	1000 ft^3 /wt%
Parameter for calculating the permeability reduction, Crk	0.0186 $\sqrt{\mathrm{darcy}}/\sqrt[3]{100\mathrm{g/g}}$
Polymer solution adsorption parameter, $a41$	0.7
Polymer solution adsorption parameter, $a42$	0.0
Polymer solution adsorption parameter, $b4$	100 ft^3 /wt%
Reacting tracer Properties	
Rate constant for a first-order aqueous phase reaction at reference temperature	0.05

Table 4.4: Summarized run cases of pressure constrained injecting field case

No	Water saturation	Polymer concentration (ppm)	Oil viscosity (cp)
1	0.35	500	4
2	0.5	500	4
3	0.65	500	4
4	0.5	1000	4
5	0.5	2000	4
6	0.5	1000	40
7	0.5	1000	100

Table 4.5: Reservoir and fluid properties of injection rate constrained field case

Reservoir Properties	
Dimensions of the five-spot	656.19 ft x 656.19 ft x 65.597 ft (200 m x 200 m x 20 m)
Number of gridblocks in the x, y and z directions	23 x 23 x 7
Gridblock sizes in the x, y, and z directions	28.53 ft x 28.53 ft x 9.371 ft
Porosity	0.3
Average permeability	15000 md
Depth of reservoir	960 m
Initial reservoir pressure	1160.9 psi
Residual water saturation	0.18
Residual oil saturation	0.3
Water viscosity	0.7 cp
Oil viscosity	80 cp
Oil density	0.855 g/cm^3
Salinity of injected water	600 ppm
Salinity of formation water	3000 ppm
Pore volume of pilot square	2.4 x 10^5 m^3
Polymer adsorption of 30% hydrolyzed polymer	18 μg/g rock
Polymer concentration at the injector	1000 ppm
Polymer viscosity	15 cp
Injecting Schedule	
Injection rate	17643.77 ft^3/day (500 m^3/day)
0.2 PV of water preflush (105 days)	
1 year of polymer injection	
0.35 PV of water postflush	

Table 4.6: Summarized run cases compared of injection rate constrained field case

No	Case description
1	30% hydrolyzed polymer injected without further hydrolysis
2	30% hydrolyzed polymer injected with further hydrolysis and its adsorption effect
3	Unhydrolyzed polymer injected with insitu polymer hydrolysis and its adsorption effect

Table 4.7: Viscosity profile comparisons in layer 4 with and without hydrolysis model

W/O Hydrolysis run (case #1)	Unhydrolyzed polymer injected W/ Hydrolysis run (case #3)

0.27 PV

0.37 PV

0.48 PV
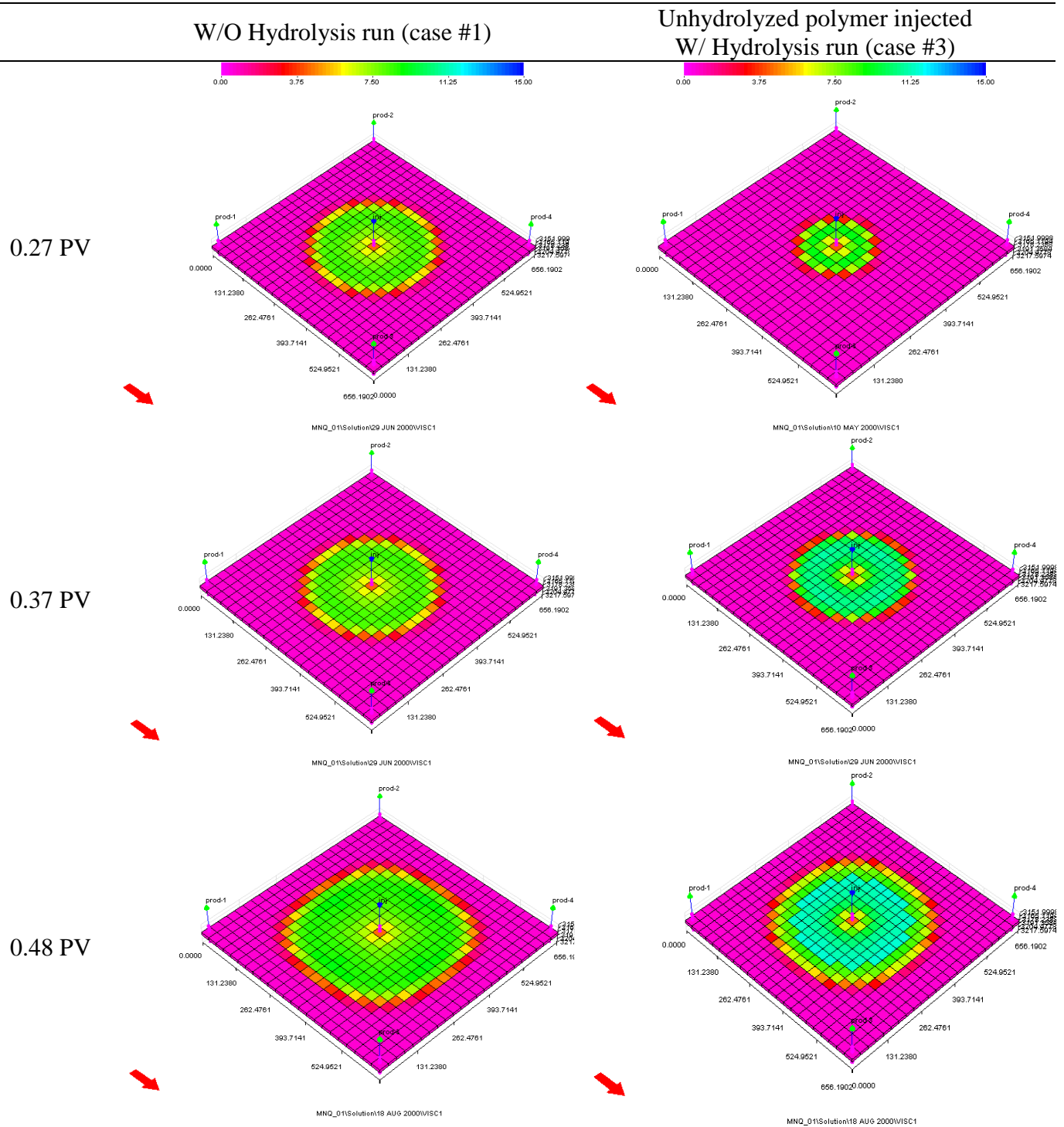
Table 4.7: Viscosity profile comparisons in layer 4 with and without hydrolysis model
(Continued)

W/O Hydrolysis run (case #1)	Unhydrolyzed polymer injected W/ Hydrolysis run (case #3)

0.58 PV

0.69 PV

0.80 PV
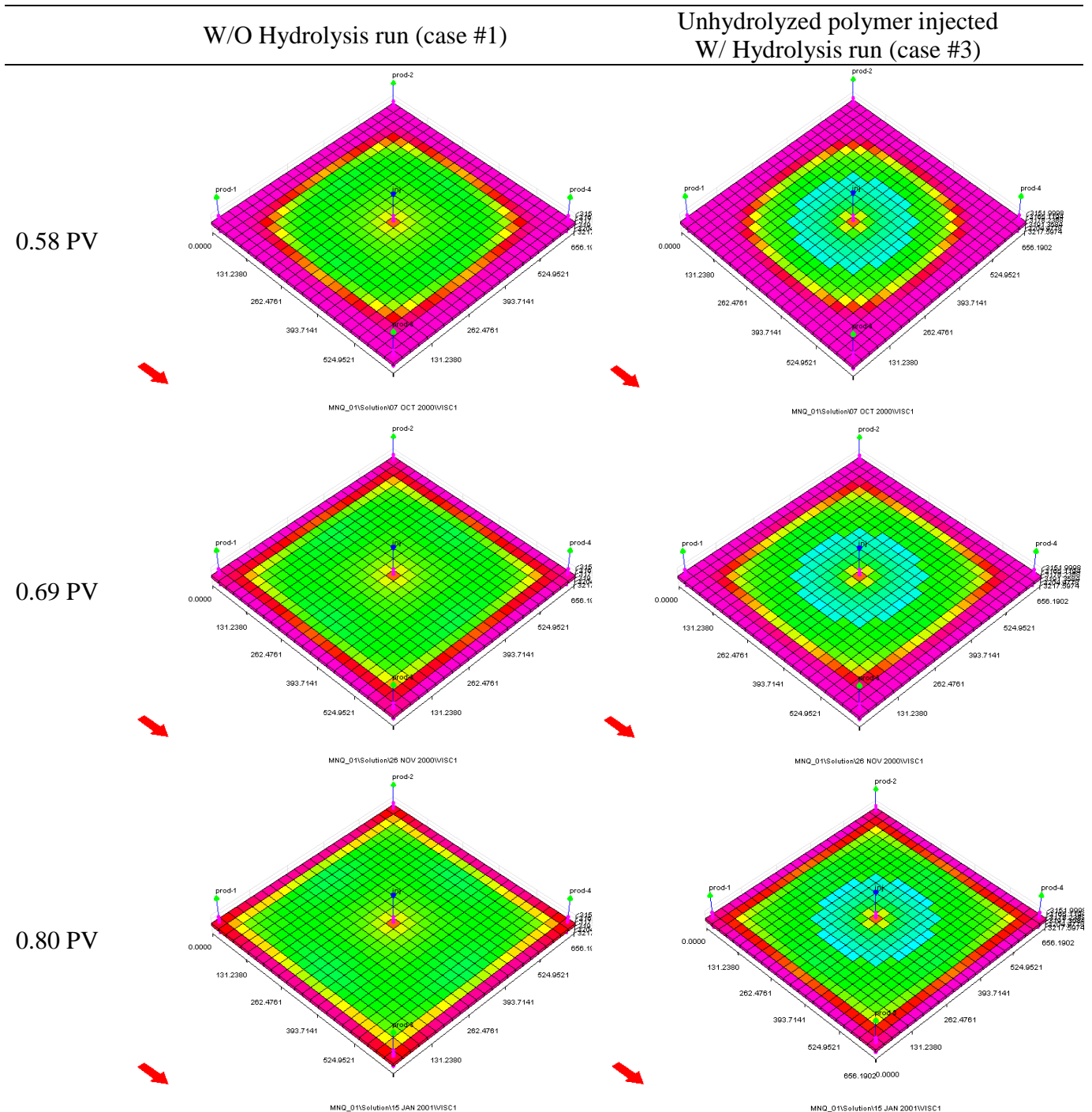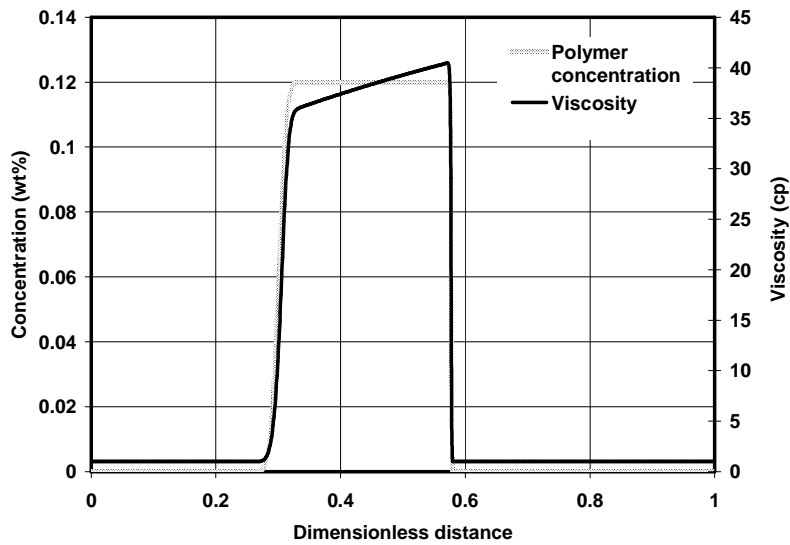
Figure 4.1(a): Simulated polymer concentration and viscosity profiles using the polymer hydrolysis model. Results are shown at 1.0 PV after injecting a   0.7 PV slug of 1200 ppm polymer concentration
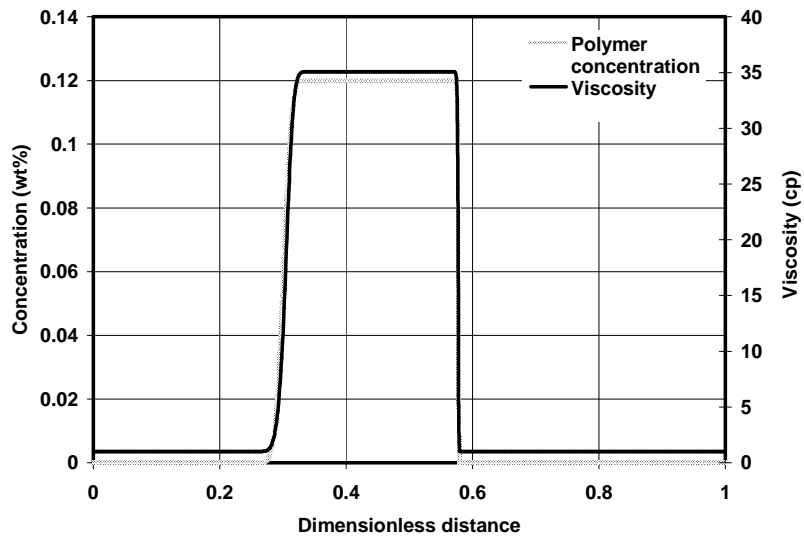
Figure 4.1(b): Polymer concentration and viscosity profile without polymer hydrolysis model at 1.0 PV injected with 0.7 PV slug of 1200 ppm polymer concentration

31
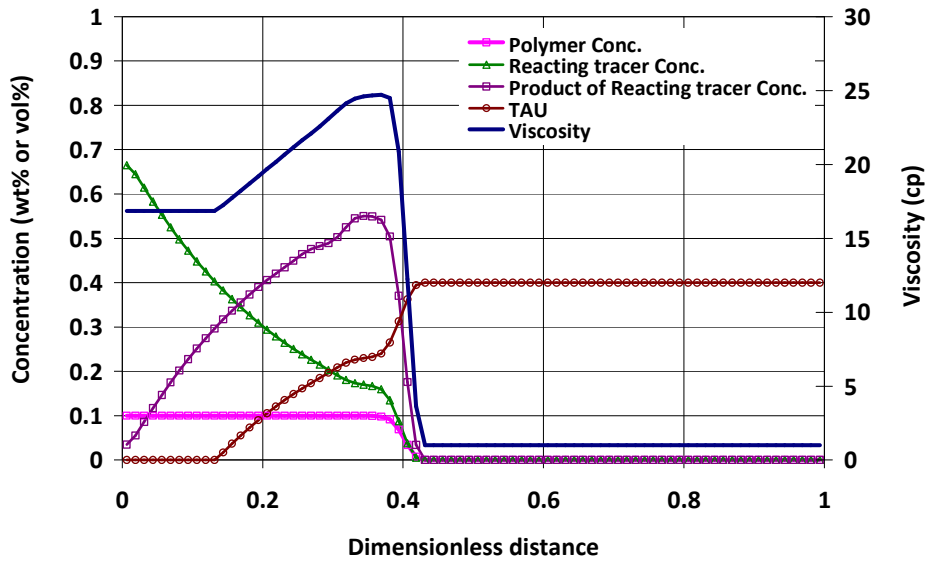
Figure 4.2(a): Concentration profiles at 0.5 PV injected with initially 30% hydrolyzed polyacrylamide injection without modeling the effect of hydrolysis on adsorption
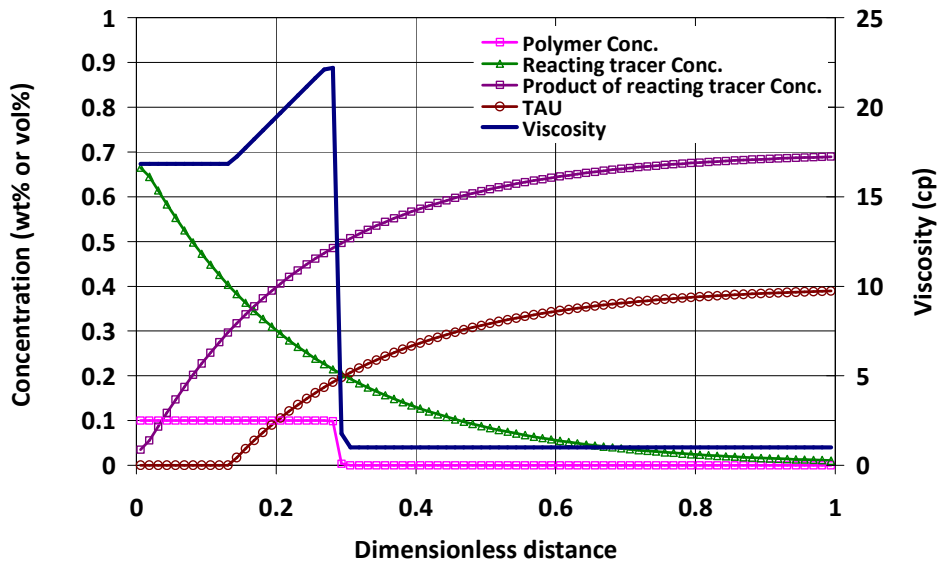
Figure 4.2(b): Concentration profiles at 3 PV injected with initially 30% hydrolyzed polyacrylamide injection with adsorption effect considered
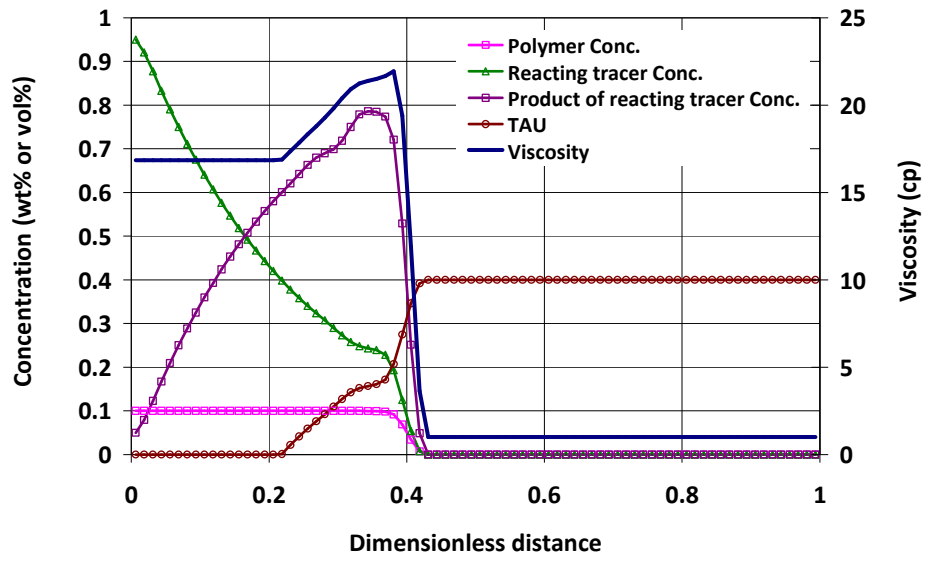
Figure 4.3(a): Concentration profiles at 0.5 PV injected with initially unhdrolyzed polyacrylamide injection without adsorption effect considered
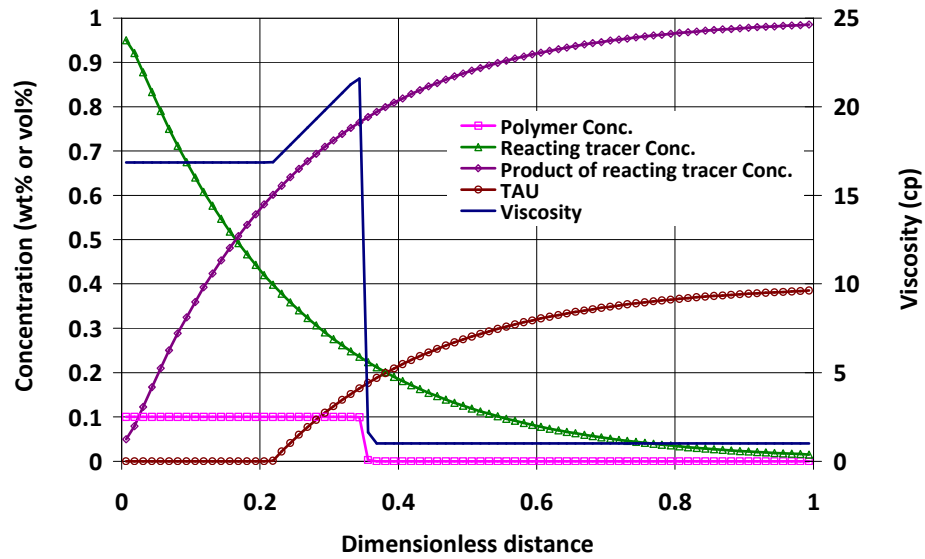
Figure 4.3(b): Concentration profiles at 10 PV injected with initially unhdrolyzed polyacrylamide injection with adsorption effect considered
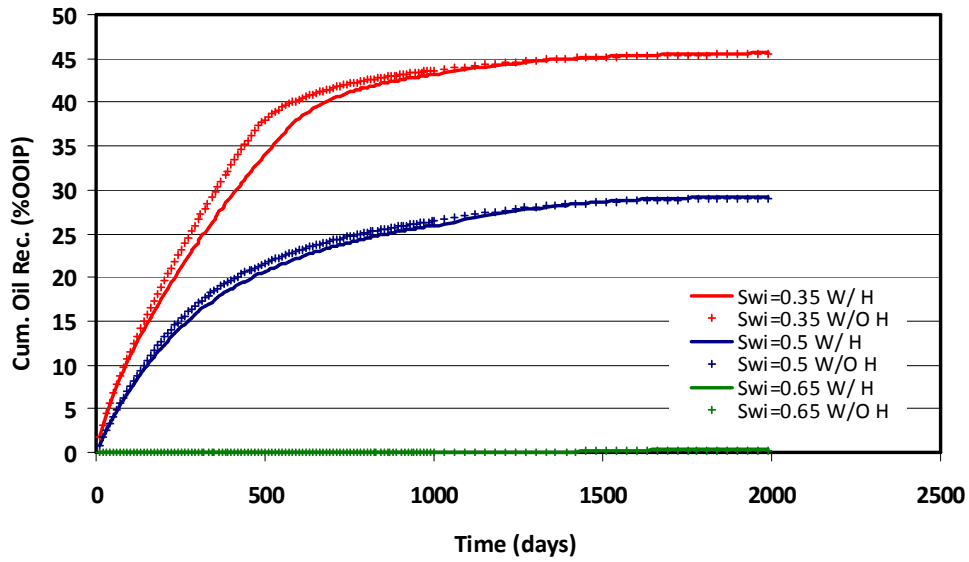
Figure 4.4(a): Cumulative oil recovery in days at different initial water saturation with polymer concentration of 500 ppm for 1000 days injection
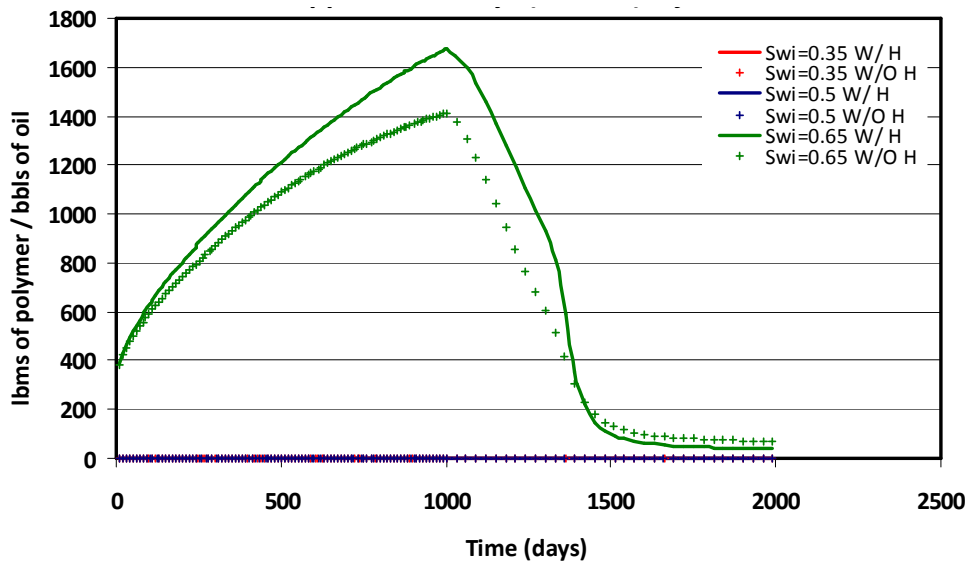
Figure 4.4(b): Injected polymer mass per bbls of oil in days at different initial water saturation with polymer concentration of 500 ppm for 1000 days of injection
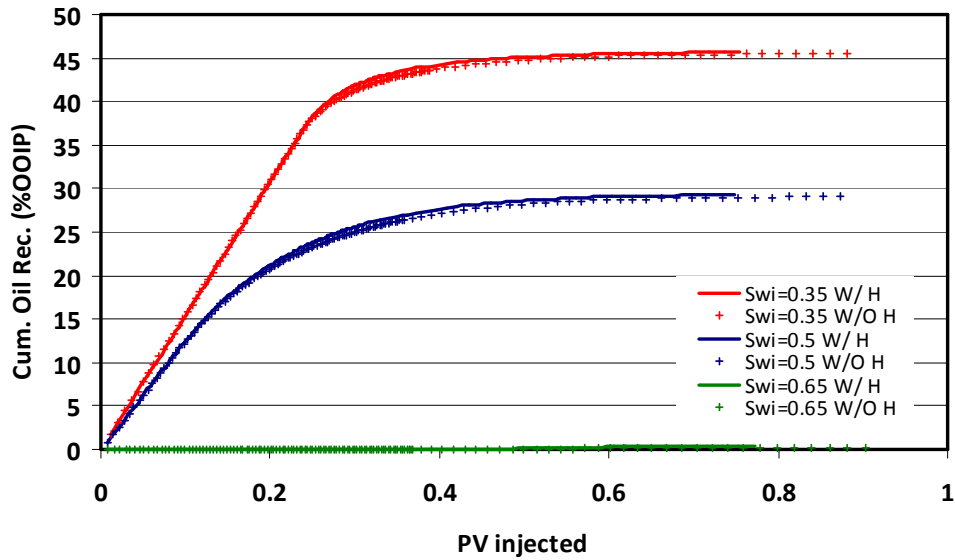
Figure 4.4(c): Cumulative oil recovery vs PV injected at different initial water saturation
with polymer concentration of 500 ppm for 1000 day injection
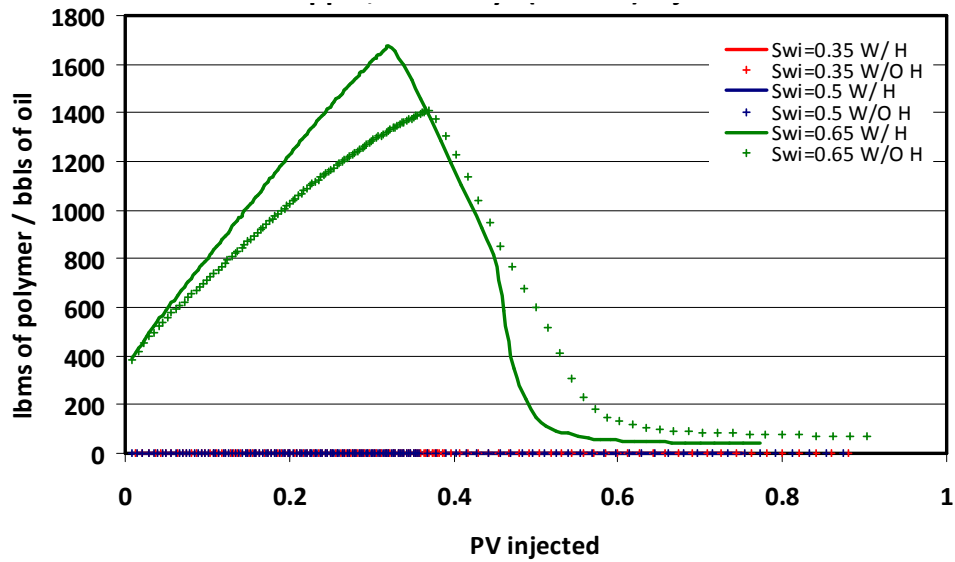
Figure 4.4(d): Injected polymer mass per bbls of oil vs PV at different initial water
saturation with polymer concentration of 500 ppm injected for 1000 days
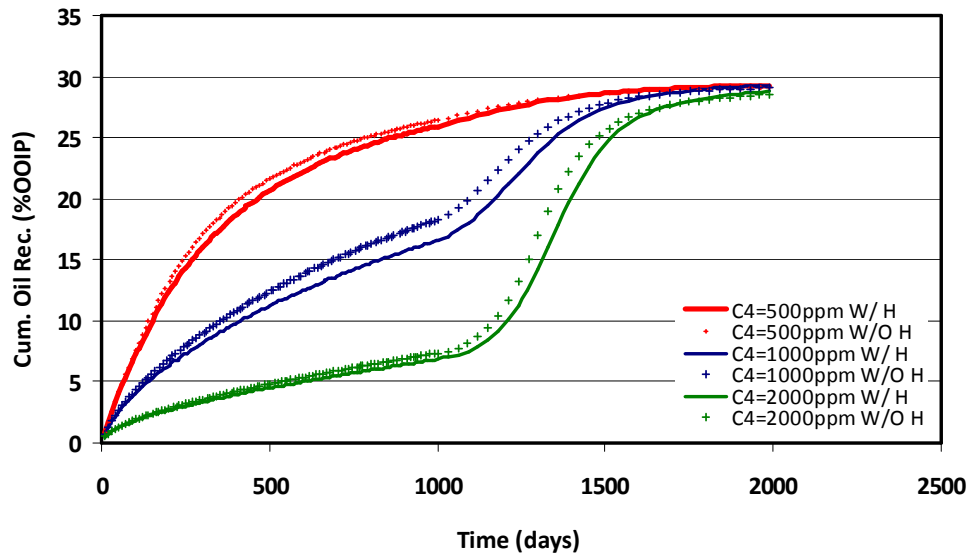
Figure 4.5(a): Cumulative oil recovery in days for different polymer concentration for 1000 days injection with initial water saturation of 0.5
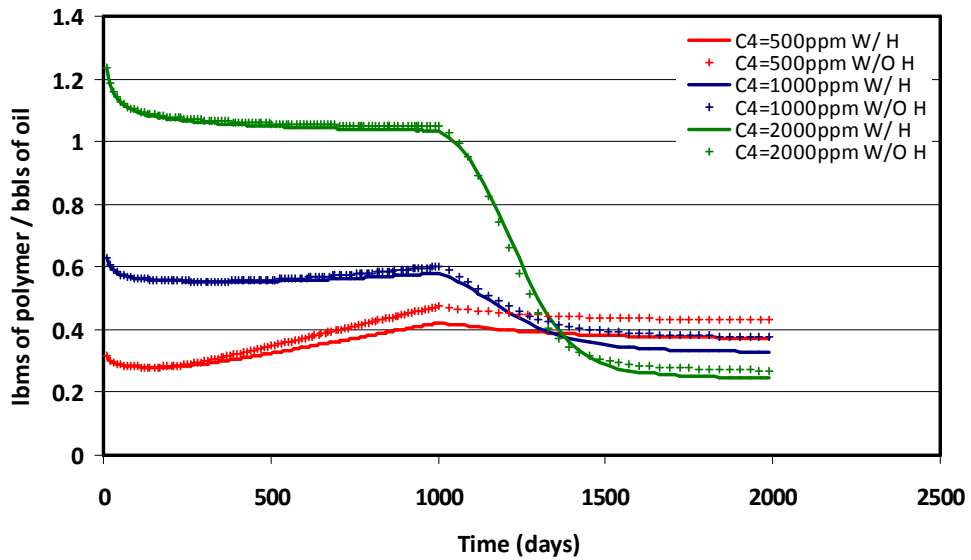
Figure 4.5(b): Injected polymer mass per bbls of oil in days at different polymer concentrations for 1000 days injection with initial water saturation of 0.5.

Cumulative Oil Recovery at different polymer concnetration @ Swi = 0.5, 1000 days (0.37 PV) injection
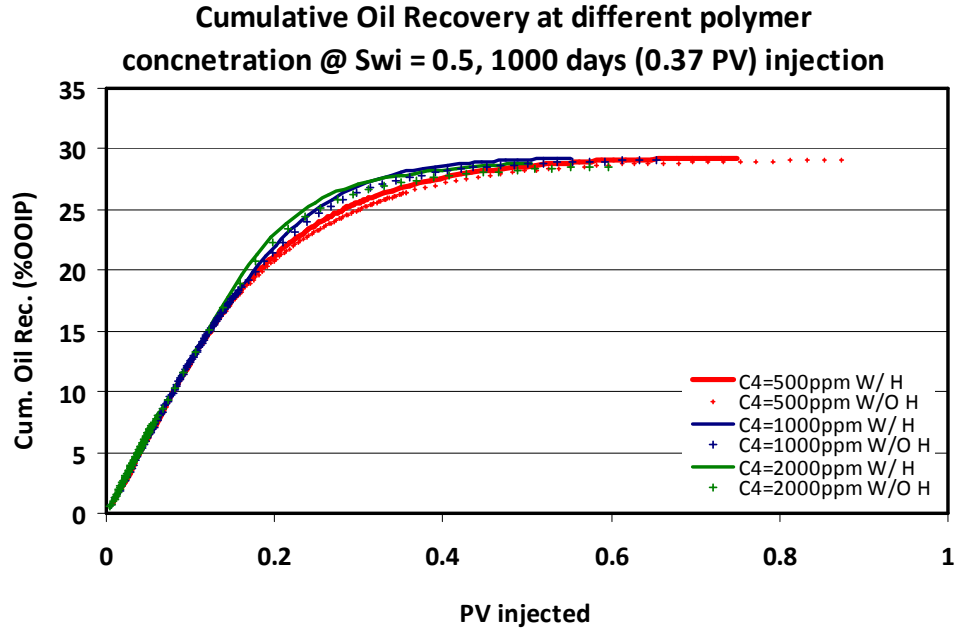
Figure 4.5(c): Cumulative oil recovery vs PV injected for different polymer concentrations for 1000 days (0.37 PV) of injection with initial water saturation of 0.5.
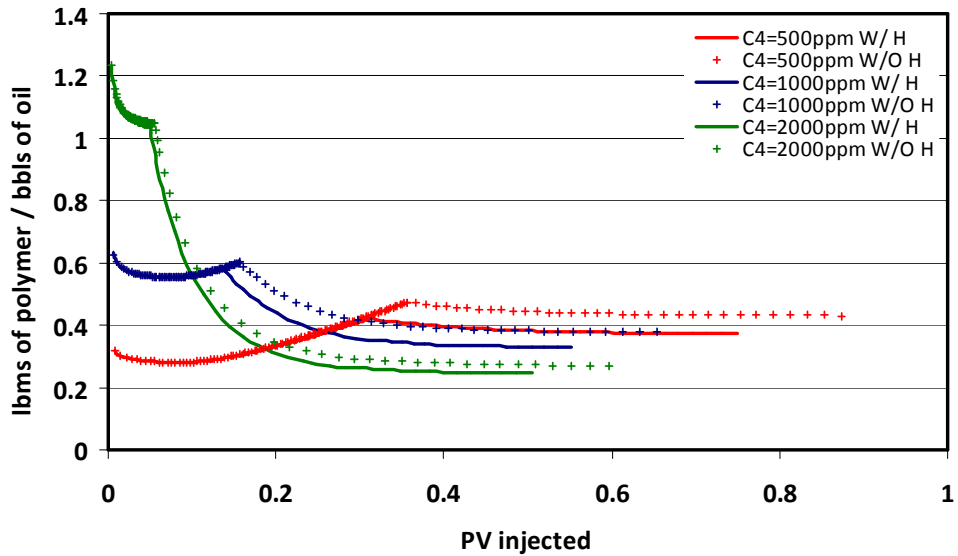
Figure 4.5(d): Injected polymer mass per bbls of oil vs PV injected for different polymer concentrations for 1000 days injection with initial water saturation of 0.5.
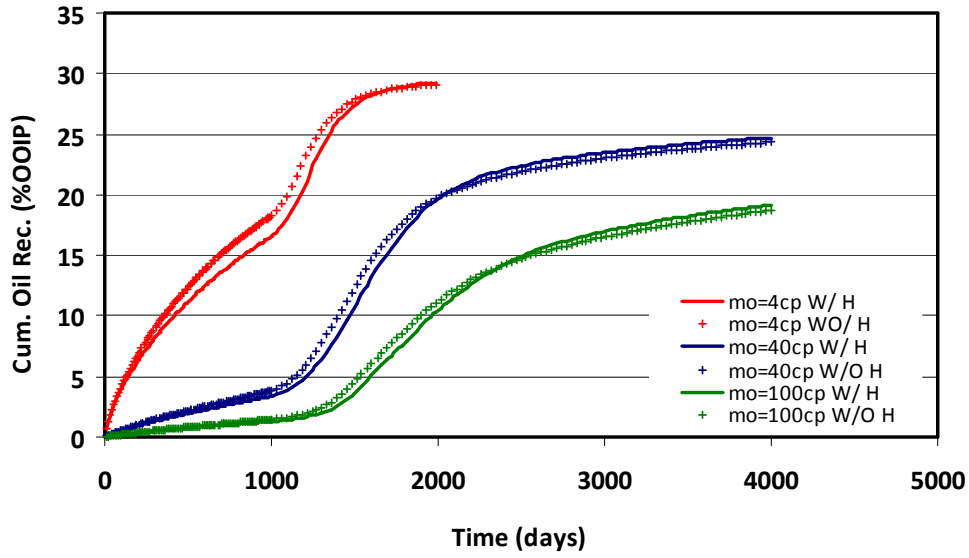
Figure 4.6(a): Cumulative oil recovery in days for different oil viscosities. Initial water saturation of 0.5 and injected polymer concentration is 1000 ppm for 4000 days injection
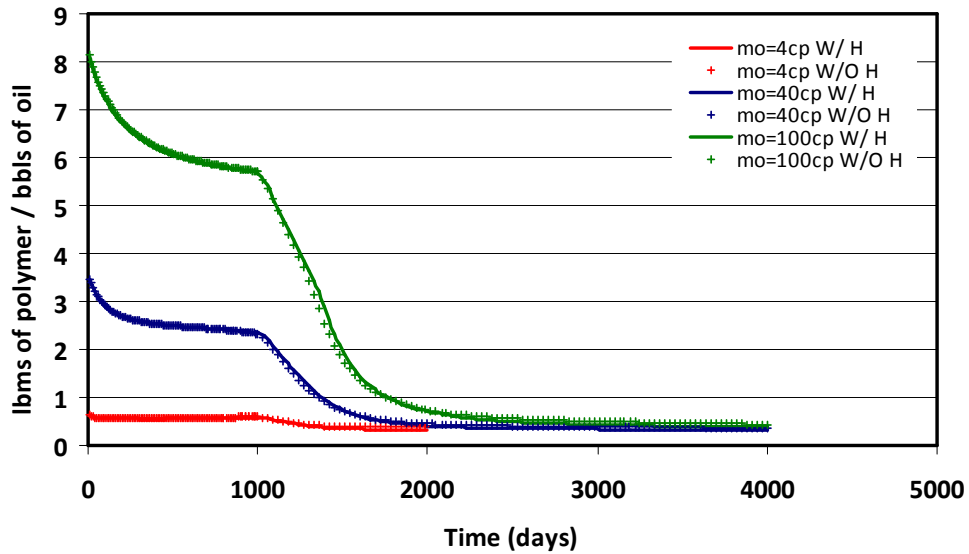
Figure 4.6(b): Injected polymer mass per bbls of oil in days for different oil viscosities. Initial water saturation is 0.5 and injected polymer concentration is 1000 ppm for 4000 days injection
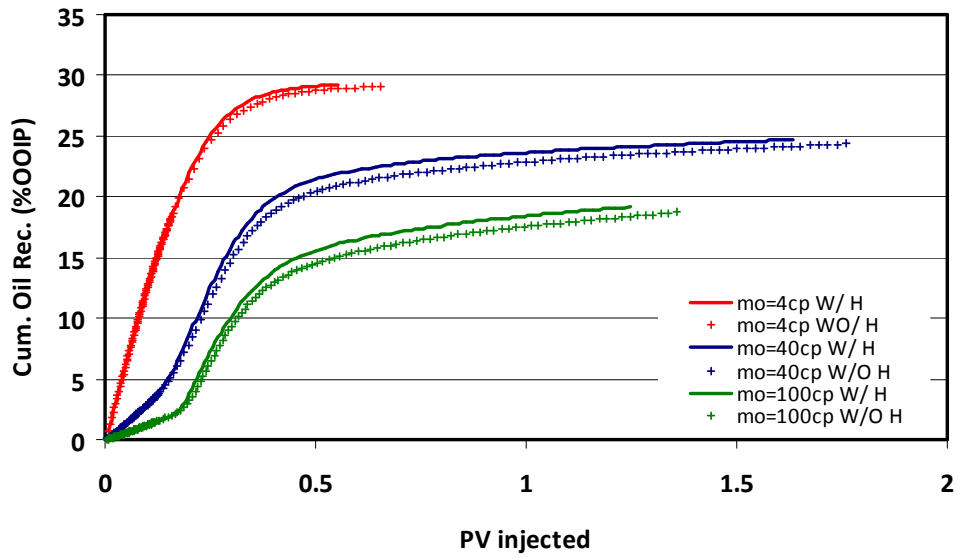
Figure 4.6(c): Cumulative oil recovery vs PV injected for different oil viscosities. Initial water saturation is 0.5 and injected polymer concentration is1000 ppm for 4000 days injection
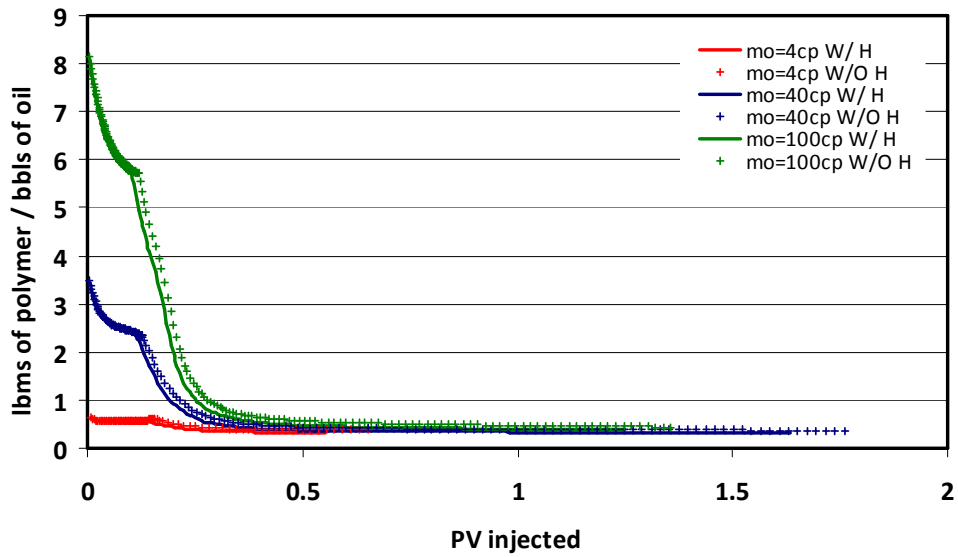
Figure 4.6(d): Injected polymer mass per bbl of oil vs PV injected for different oil viscosities. Initial water saturation is 0.5 and injected polymer concentration is 1000 ppm for 4000 days injection
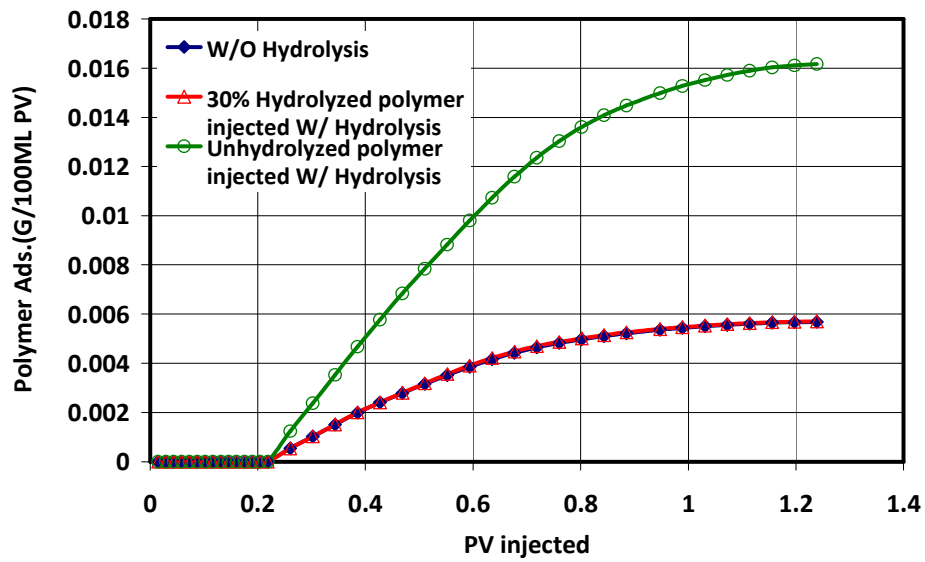
Figure 4.7: Polymer adsorption vs PV injected
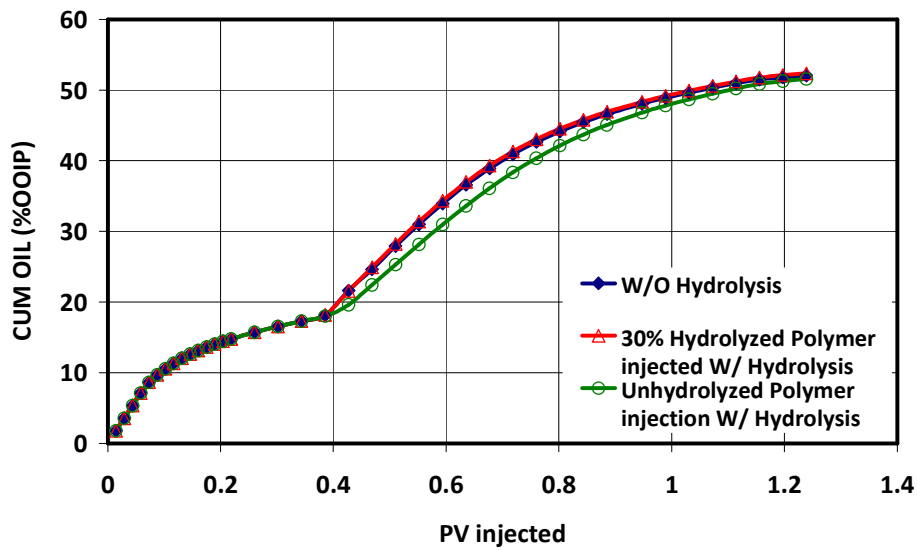
Figure 4.8: Cumulative oil recovery vs PV injected
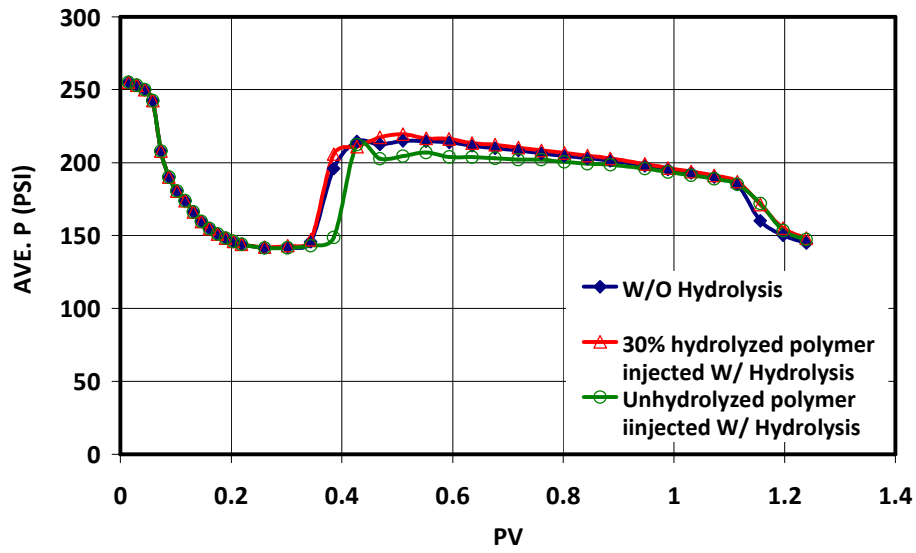
Figure 4.9: Average reservoir pressure for each case in PV injected
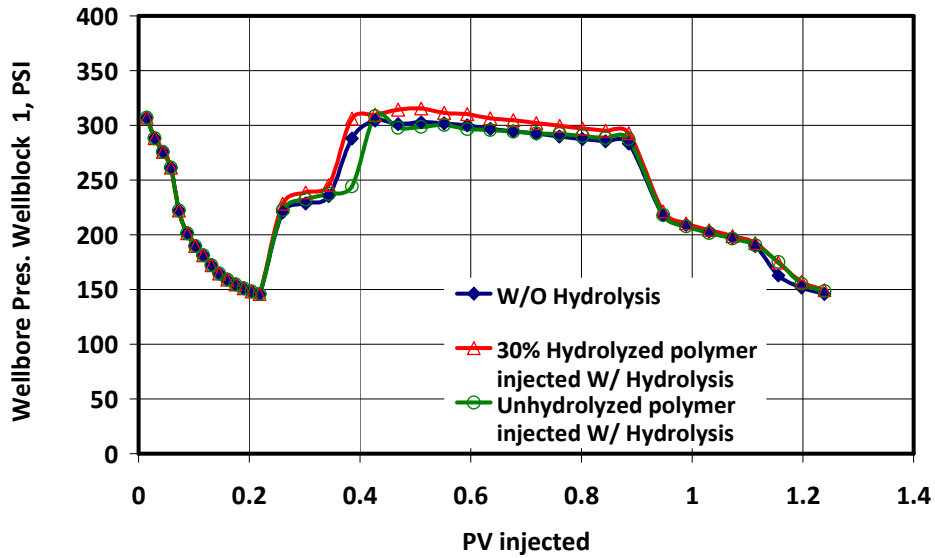
Figure 4.10: Reservoir pressure at near wellbore fort each case in PV injected

Chapter 5: SUMMARY AND CONCLUSIONS

This study focused on the development and implementation of a polymer hydrolysis model into a chemical flooding simulator for enhanced oil recovery called UTCHEM, and the illustration of the model through simulations. The following summary and conclusions are derived.

1. The polyacrylamide polymer hydrolysis due to anionically charged carboxyl groups induces extension of the molecules through electrostatic repulsion among the chain, therby increasing viscosity. The degree of hydrolysis increases as time passes, and the viscosity also increases as the degree of hydrolysis increases.

2. Polymer hydrolysis model was developed based on literature research;

$$\left[\frac{d\tau}{dt}\right]_H = k(1-\tau)^{1.6}$$

$$\Lambda_p = \frac{1}{1-1.4335\tau}$$

where, τ is the degree of hydrolysis in fraction, $t=0$ is time, k is the reaction rate, and Λ_p is the ratio of the intrinsic viscosity of PAM and HPAM.

3. The developed model was implemented in UTCHEM, the chemical flooding simulator developed in the University of Texas at Austin, as one of the running options. The running option can be turned on and off as the polymer hydrolysis effect is considered or not.

4. 1D coreflood simulation demonstrated the viscosity change affected by the polymer hydrolysis. While polymer concentration exists, the viscosity increases along the core.

5. In a quarter of five-spot field reservoir simulation, the pressure constrained injector case shows that injected amount of polymer reduced when polymer hydrolysis is considered even though oil recovery was not changed much compared with the previously simulated results.

6. The polymer flooding with adsorption in a five-spot pattern reservoir was simulated with injection rate constrained injector. Hydrolyzed polymer and unhydrolyzed polymer were used to simulate polymer hydrolysis and adsorption effect. On early time polymer spreads widely for hydrolyzed polymer injection case because of its lower value of adsorption, however, as time passes polymer viscosity increased more for unhydrolyzed polymer injection case because of its hydrolysis effect in the reservoir.

7. Polymer hydrolysis of initially unhydrolyzed polymer in the reservoir is noticeable since the aqueous phase viscosity increases more with lower average reservoir pressure than HPAM even with higher polymer adsorption for unhydrolyzed polymer.

Appendix A: UTCHEM Input File with Polymer Hydrolysis Model

This is UTCHEM input file for polymer flooding with polymer hydrolysis model considered using unhydrolyzed polymer with adsorption and injection rate constrained injection applied.

```
CC*********************************************************************
CC                                                                    *
CC    BRIEF DESCRIPTION OF DATA SET : UTCHEM (VERSION 9.95)           *
CC                                                                    *
CC*********************************************************************
CC  WATER OR POLYMER FLOOD FOR CHATEAUNARD FULL FIELD 15X15X3         *
CC                                                                    *
CC  LENGTH (FT) : 656.2           PROCESS :  POLYMER FLOOD            *
CC  THICKNESS (FT) : 65.6          INJ. RATE (FT3/DAY) : 17643.77     *
CC  WIDTH (FT) : 656.2                                                *
CC  POROSITY : 0.30               COORDINATES : CARTESIAN             *
CC  GRID BLOCKS : 23x23x7          PERMEABILITY :constant permeability *
CC  DATE : 09/09/10                                                   *
CC                                                                    *
CC                                                                    *
CC*********************************************************************
CC
CC*********************************************************************
CC                                                                    *
CC    RESERVOIR DESCRIPTION                                           *
CC                                                                    *
CC*********************************************************************
CC
CC Run number
*---- RUNNO
INJCPH
CC
CC Title and run description
*---- title(i)
polymer flood with injection rate constrained


CC
CC SIMULATION FLAGS
*---IMODE IMES IDISPC ICWM ICAP IREACT IBIO ICOORD ITREAC ITC IGAS IENG
     1    2     2     0    0    0     0    1      1     0   0    0
CC
CC no. of gridblocks,flag specifies constant or variable grid size,unit
*---- NX    NY    NZ  IDXYZ  IUNIT
      23    23    7     0      0
CC
CC constant grid block size in x,y,and z
*---- dx1          dy1          dz1
     28.53        28.53        9.371
CC
CC total no. of components,no. of tracers,no. of gel components
```

```
*----n    no    ntw    nta    ngc    ng    noth
    11   0     3      0      0      0     0
CC
CC Name of the components
*----spname(i) for i=1 to n
Water
Oil
NONE
Polymer
Chloride
Calcium
NONE
NONE
Tracer 1 - Nonreacting Tracer
Reacting tracer
Product of Reacting Tracer
CC
CC FLAG INDICATING THE UNITS OF INJECTED TRACERS ( 1 = VOL% , 2 = WT% )
*----ITRU(IT) FOR IT=1,NTW
    1 1 1
CC
CC flag indicating if the component is included in calculations or not
*----icf(kc) for kc=1,n
    1 1 0 1 1 1 0 0 1 1 1
CC
CC***************************************************************
CC                                                             *
CC    OUTPUT OPTIONS                                           *
CC                                                             *
CC***************************************************************
CC
CC
CC FLAG TO WRITE TO UNIT 3,FLAG FOR PV OR DAYS TO PRINT OR TO STOP THE
RUN
*---- ICUMTM  ISTOP  IOUTGMS
      0       0      0
CC
CC FLAG INDICATING IF THE PROFILE OF KCTH COMPONENT SHOULD BE WRITTEN
*---- IPRFLG(KC),KC=1,N
    1 1 0 1 1 1 0 0 1 1 1
CC
CC FLAG FOR PRES.,SAT.,TOTAL CONC.,TRACER CONC.,CAP.,GEL, ALKALINE
PROFILES
*---- IPPRES IPSAT IPCTOT IPBIO IPCAP IPGEL IPALK IPTEMP IPOBS
      1      1     1      0     0     0     0     0      0
CC
CC FLAG FOR WRITING SEVERAL PROPERTIES TO UNIT 4 (Prof)
*---- ICKL IVIS IPER ICNM ICSE IHYSTP IFOAMP INONEQ
      1    1    0    0    1    0      0      0
CC
CC FLAG  for variables to PROF output file
*---- IADS IVEL IRKF IPHSE
      1    1    1    0
CC
CC***************************************************************
CC                                                             *
CC    RESERVOIR PROPERTIES                                     *
CC                                                             *
CC***************************************************************
CC
```

45

```
CC
CC MAX. SIMULATION TIME ( DAYS)
*---- TMAX
      600
CC
CC ROCK COMPRESSIBILITY (1/PSI), STAND. PRESSURE(PSIA)
*---- COMPR        PSTAND
        0           1000
CC
CC FLAGS INDICATING CONSTANT OR VARIABLE POROSITY, X,Y,AND Z
PERMEABILITY
*---- IPOR1  IPERMX  IPERMY  IPERMZ  IMOD    ITRNZ   INTG
        0       0       0       0       0       0       0
CC
CC constant porosity
*---- PORC1
      0.3
CC
CC CONSTANT X-PERMEABILITY (MILIDARCY) FOR LAYER K = 1,NZ
*----PERMXC
    15000
CC
CC Y DIRECTION PERMEABILITY IS DEPENDENT ON X DIRECTION PERMEABILITY
*---- PERMYC
    15000
CC
CC CONSTANT Z-PERMEABILITY (MILIDARCY) FOR LAYER K = 1,NZ
*----PERMZC
    15000
CC
CC FLAG FOR CONSTANT OR VARIABLE DEPTH, PRESSURE, WATER
SATURATION,INITIAL AQUEOUS PHASE COMPOSITIONS
*----IDEPTH  IPRESS  ISWI  ICWI
      0       0       0     -1
CC
CC CONSTANT DEPTH (FT)
*---- D111
      3151.67
CC
CC CONSTANT PRESSURE (PSIA)
*---- PRESS1
      1160.9
CC
CC CONSTANT INITIAL WATER SATURATION
*---- SWI
      0.18
CC
CC BRINE SALINITY AND DIVALENT CATION CONCENTRATION (MEQ/ML)
*---- C50       C60
      0.0513   0.001
CC
CC********************************************************************
CC                                                                  *
CC    PHYSICAL PROPERTY DATA                                        *
CC                                                                  *
CC********************************************************************
CC
CC
CC OIL CONC. AT PLAIT POINT FOR TYPE II(+)AND TYPE II(-), CMC
*---- c2plc  c2prc   epsme   ihand
```

```
         0     1     0.0001    0
CC
CC flag indicating type of phase behavior parameters
*---- ifghbn
        0
CC SLOPE AND INTERCEPT OF BINODAL CURVE AT ZERO, OPT., AND 2XOPT
SALINITY
CC FOR ALCOHOL 1
*---- hbns70   hbnc70   hbns71   hbnc71   hbns72   hbnc72
       0.131    0.1      0.191    0.026    0.363    0.028
CC SLOPE AND INTERCEPT OF BINODAL CURVE AT ZERO, OPT., AND 2XOPT
SALINITY
CC FOR ALCOHOL 2
*---- hbns80  hbnc80  hbns81  hbnc81  hbns82  hbnc82
        0       0       0       0       0       0
CC
CC LOWER AND UPPER EFFECTIVE SALINITY FOR ALCOHOL 1 AND ALCOHOL 2
*---- csel7   cseu7   csel8   cseu8
      0.177   0.344    0       0
CC
CC THE CSE SLOPE PARAMETER FOR CALCIUM AND ALCOHOL 1 AND ALCOHOL 2
*---- beta6    beta7    beta8
       6        -2        0
CC
CC FLAG FOR ALCOHOL PART. MODEL AND PARTITION COEFFICIENTS
*---- ialc   opsk7o   opsk7s   opsk8o   opsk8s
       1       0        0        0        0
CC
CC NO. OF ITERATIONS, AND TOLERANCE
*---- nalmax     epsalc
       20        0.001
CC
CC ALCOHOL 1 PARTITIONING PARAMETERS IF IALC=1
*---- akwc7    akws7    akm7    ak7     pt7
      4.671    1.79     48     35.31    0.222
CC
CC ALCOHOL 2 PARTITIONING PARAMETERS IF IALC=1
*---- akwc8    akws8    akm8    ak8     pt8
       0        0        0       0       0
CC
CC ift model flag
*---- ift
        0
CC
CC INTERFACIAL TENSION PARAMETERS
*---- g11     g12     g13     g21     g22     g23
      13     -14.8    0.007    13    -14.5    0.01
CC
CC LOG10 OF OIL/WATER INTERFACIAL TENSION
*---- xiftw
      1.3
CC
CC ORGANIC MASS TRANSFER FLAG
*---- imass icor
        0      0
CC
CC
*--- iwalt  iwalf
      0     0
CC
```

```
CC CAPILLARY DESATURATION PARAMETERS FOR PHASE 1, 2, AND 3
*---- itrap      t11      t22      t33
       0        0        0     364.2
CC
CC  FLAG FOR RELATIVE PERMEABILITY AND CAPILLARY PRESSURE MODEL
*---- iperm     IRTYPE
       0         0
CC
CC FLAG FOR CONSTANT OR VARIABLE REL. PERM. PARAMETERS
*---- isrw    iprw    iew
       0       0       0
CC
CC CONSTANT RES. SATURATION OF PHASES 1,2,AND 3 AT LOW CAPILLARY NO.
*---- s1rwc    s2rwc    s3rwc
       0.18     0.3      0
CC
CC CONSTANT ENDPOINT REL. PERM. OF PHASES 1,2,AND 3 AT LOW CAPILLARY
NO.
*---- p1rwc     p2rwc    p3rwc
       0.3       0.8      0.2
CC
CC CONSTANT REL. PERM. EXPONENT OF PHASES 1,2,AND 3 AT LOW CAPILLARY
NO.
*---- e1wc     e2wc     e3wc
       2        2        1
CC
CC WATER AND OIL VISCOSITY , RESERVOIR TEMPERATURE
*---- VIS1    VIS2    TSTAND
       0.7     80       0
CC
CC COMPOSITIONAL PHASE VISCOSITY PARAMETERS
*---- ALPHAV1   ALPHAV2   ALPHAV3   ALPHAV4  ALPHAV5
       4         5         0         0.9       0.7
CC
CC PARAMETERS TO CALCULATE POLYMER VISCOSITY AT ZERO SHEAR RATE
*---- AP1      AP2      AP3
      13.5      350      400
CC
CC PARAMETER TO COMPUTE CSEP,MIN. CSEP, AND SLOPE OF LOG VIS. VS. LOG
CSEP
*---- BETAP    CSE1     SSLOPE
       6       0.0553    -0.38
CC
CC PARAMETER FOR SHEAR RATE DEPENDENCE OF POLYMER VISCOSITY
*---- GAMMAC   GAMHF   POWN     IPMOD   ishear  rweff    IPHYDRO
       3.97     6       1.8      0       0       0.25      1
CC
CC When IPHYDRO=1,
*---- EHDR      CHDR1     CHDR2      REVTEMP
       1.6      91.3      27.149     200.0
CC
CC CC FLAG FOR POLYMER PARTITIONING, PERM. REDUCTION PARAMETERS
*---- IPOLYM    EPHI3    EPHI4    BRK     CRK     RKCUT
       1        0.85     0.85     100     0.23     10
CC
CC SPECIFIC WEIGHT FOR COMPONENTS 1,2,3,7,8 ,Coeffient of oil and
GRAVITY FLAG
*---- DEN1       DEN2        DEN23       DEN3     DEN7     DEN8    IDEN
     0.43353    0.385839    0.385839    0.42     0.346     0        2
CC
```

```
CC FLAG FOR CHOICE OF UNITS ( 0:BOTTOMHOLE CONDITION , 1: STOCK TANK)
*----- ISTB
        0
CC
CC COMPRESSIBILITY FOR VOL. OCCUPYING COMPONENTS 1,2,3,7,AND 8
*---- COMPC(1) COMPC(2) COMPC(3) COMPC(7) COMPC(8)
        0       0       0       0       0
CC
CC CONSTANT OR VARIABLE PC PARAM., WATER-WET OR OIL-WET PC CURVE FLAG
*---- ICPC   IEPC   IOW
        0      0      0
CC
CC CAPILLARY PRESSURE PARAMETER, CPC0
*---- CPC0
        0
CC
CC CAPILLARY PRESSURE PARAMETER, EPC0
*---- EPC0
        2
CC
CC MOLECULAR DIFFUSION COEF. KCTH COMPONENT IN PHASE 1
*---- D(KC,1),KC=1,N
        11*0.
CC
CC MOLECULAR DIFFUSION COEF. KCTH COMPONENT IN PHASE 2
*---- D(KC,2),KC=1,N
        11*0.
CC
CC MOLECULAR DIFFUSION COEF. KCTH COMPONENT IN PHASE 3
*---- D(KC,3),KC=1,N
        11*0.
CC
CC LONGITUDINAL AND TRANSVERSE DISPERSIVITY OF PHASE 1
*---- ALPHAL(1)   ALPHAT(1)
        1          0
CC
CC LONGITUDINAL AND TRANSVERSE DISPERSIVITY OF PHASE 2
*---- ALPHAL(2)    ALPHAT(2)
        1          0
CC
CC LONGITUDINAL AND TRANSVERSE DISPERSIVITY OF PHASE 3
*---- ALPHAL(3)    ALPHAT(3)
        0          0
CC
CC flag to specify organic adsorption calculation
*---- iadso
        0
CC
CC SURFACTANT AND POLYMER ADSORPTION PARAMETERS
*---- AD31   AD32   B3D   AD41   AD42   B4D   IADK   IADS1  FADS   REFK
      1     0.5   1000   3.54    0    100    0      0      0      0
CC
CC PARAMETERS FOR CATION EXCHANGE OF CLAY AND SURFACTANT
*---- QV  XKC   XKS    EQW
      0   0    0      419
CC
CC TRACER PARTITIONING COEFFICIENT (TK(IT),IT=1,NT)
*---- TK(1)  TK(2)  TK(3)
      0.0    0.0    0.0
CC
```

49

```
CC TRACER PARTITION COEFFICIENT SALINITY PARAMETER (1/MEQ/ML)
*----TKS(IT), IT=1,NT      C5INI
      0.0    0.0      0.0    0.0
CC
CC RADIACTIVE DECAY COEFFICIENT (RDC(IT),IT=1,NT)
*---- RDC(1)  RDC(2)   RDC(3)
      0.0      0.0       0.0
CC
CC TRACER RETARDATION COEFFICIENT (RET(IT),IT=1,NT)
*---- RET(1)   RET(2)  RET(3)
      0.0      0.0       0.0
CC
cc tracer reaction
*--- NRT     TAK(1)
     1       0.5
CC
CC TRACER MOLECULAR WEIGHT  (TMW(IT),IT=1,NT)
*---- TMW(1)  TMW(2)   TMW(3)
      1.0    1.0      1.0
CC
CC TRACER DENSITY IN G/CC (TDEN(IT),IT=1,NT)
*---- TDEN(1)  TDEN(2)   TDEN(3)
      1.0    1.0      1.0
CC
CC*******************************************************************
CC                                                                 *
CC    WELL DATA                                                    *
CC                                                                 *
CC*******************************************************************
CC
CC
CC FLAG FOR SPECIFIED BOUNDARY AND ZONE IS MODELED
*---- IBOUND     IZONE
       0      0
CC
CC TOTAL NUMBER OF WELLS, WELL RADIUS FLAG, FLAG FOR TIME OR COURANT
NO.
*---- NWELL    IRO    ITIME    NWREL
       5     1     1        5
CC
CC WELL ID,LOCATIONS,AND FLAG FOR SPECIFYING WELL TYPE, WELL RADIUS,
SKIN
*---- IDW   IW   JW   IFLAG   RW    SWELL  IDIR  IFIRST  ILAST  IPRF
     1    12   12    1   0.2864   0      3      1       7       0
CC
CC WELL NAME
*---- WELNAM
inj
CC
CC ICHEK , MAX. AND MIN. ALLOWABLE BOTTOMHOLE PRESSURE AND RATE
*---- ICHEK     PWFMIN     PWFMAX    QTMIN    QTMAX
       0        0        30000     0        9000
CC
CC WELL ID,LOCATIONS,AND FLAG FOR SPECIFYING WELL TYPE, WELL RADIUS,
SKIN
*---- IDW  IW  JW  IFLAG  RW   SWELL  IDIR  IFIRST  ILAST  IPRF
      2   1   1    2  0.2864   0      3      1       7       0
CC
CC WELL NAME
*---- WELNAM
```

```
prod-1
CC
CC ICHEK , MAX. AND MIN. ALLOWABLE BOTTOMHOLE PRESSURE AND RATE
*---- ICHEK     PWFMIN    PWFMAX    QTMIN    QTMAX
       0         0        30000      0       50000
CC
CC WELL ID,LOCATIONS,AND FLAG FOR SPECIFYING WELL TYPE, WELL RADIUS,
SKIN
*---- IDW   IW   JW   IFLAG   RW    SWELL  IDIR  IFIRST  ILAST  IPRF
       3    1    23    2    0.2864   0      3      1       7      0
CC
CC WELL NAME
*---- WELNAM
prod-2
CC
CC ICHEK , MAX. AND MIN. ALLOWABLE BOTTOMHOLE PRESSURE AND RATE
*---- ICHEK     PWFMIN    PWFMAX    QTMIN    QTMAX
       0         0        30000      0       50000
CC
CC WELL ID,LOCATIONS,AND FLAG FOR SPECIFYING WELL TYPE, WELL RADIUS,
SKIN
*---- IDW   IW   JW   IFLAG   RW    SWELL  IDIR  IFIRST  ILAST  IPRF
       4    23   1     2    0.2864   0      3      1       7      0
CC
CC WELL NAME
*---- WELNAM
prod-3
CC
CC ICHEK , MAX. AND MIN. ALLOWABLE BOTTOMHOLE PRESSURE AND RATE
*---- ICHEK     PWFMIN    PWFMAX    QTMIN    QTMAX
       0         0        30000      0       50000
CC
CC WELL ID,LOCATIONS,AND FLAG FOR SPECIFYING WELL TYPE, WELL RADIUS,
SKIN
*---- IDW   IW   JW   IFLAG   RW    SWELL  IDIR  IFIRST  ILAST  IPRF
       5    23   23    2    0.2864   0      3      1       7      0
CC
CC WELL NAME
*---- WELNAM
prod-4
CC
CC ICHEK , MAX. AND MIN. ALLOWABLE BOTTOMHOLE PRESSURE AND RATE
*---- ICHEK     PWFMIN    PWFMAX    QTMIN    QTMAX
       0         0        30000      0       50000
CC
CC  ID,INJ. RATE AND INJ. COMP. FOR RATE CONS. WELLS FOR EACH PHASE
(L=1,3)
*---- ID   QI(M,L)    C(M,KC,L)
       1  17643.776  1   0   0   0  0.0533  0.001  0   0   0  1.0   0
       1   0         0   0   0   0   0       0     0   0   0   0
       1   0         0   0   0   0   0       0     0   0   0   0
CC
CC ID, BOTTOM HOLE PRESSURE FOR PRESSURE CONSTRAINT WELL (IFLAG=2 OR 3)
*---- ID    PWF
       2    100
CC
CC ID, BOTTOM HOLE PRESSURE FOR PRESSURE CONSTRAINT WELL (IFLAG=2 OR 3)
*---- ID    PWF
       3    100
CC
```

```
CC ID, BOTTOM HOLE PRESSURE FOR PRESSURE CONSTRAINT WELL (IFLAG=2 OR 3)
*---- ID    PWF
      4     100
CC
CC ID, BOTTOM HOLE PRESSURE FOR PRESSURE CONSTRAINT WELL (IFLAG=2 OR 3)
*---- ID    PWF
      5     100
CC
CC CUM. INJ. TIME , AND INTERVALS (PV OR DAY) FOR WRITING TO OUTPUT
FILES
*---- TINJ      CUMPR1    CUMHI1    WRHPV    WRPRF    RSTC
      105       10        10        7        68       100
CC
CC THE INI. TIME STEP,CONC. TOLERANCE,MAX.,MIN. time steps
*---- DT
      0.0001  0.001 0.4 .04
CC
CC FLAG FOR INDICATING BOUNDARY CHANGE
*---- IBMOD
      0
CC
CC IRO, ITIME, NEW FLAGS FOR ALL THE WELLS
*---- IRO    ITIME    IFLAG
      1      0        1     2     2     2     2
CC
CC NUMBER OF WELLS CHANGES IN LOCATION OR SKIN OR PWF
*---- NWEL1
      0
CC
CC NUMBER OF WELLS WITH RATE CHANGES, ID
*---- NWEL2     ID
      1         1
CC
CC ID,INJ. RATE AND INJ. COMP. FOR RATE CONS. WELLS FOR EACH PHASE
(L=1,3)
*---- ID   QI(M,L)   C(M,KC,L)
      1 17643.776   1  0  0 0.1 0.0553 0.001 0  0  0 1.0  0
      1  0         0  0  0  0  0      0     0  0  0  0  0
      1  0         0  0  0  0  0      0     0  0  0  0  0
CC
CC CUM. INJ. TIME , AND INTERVALS (PV) FOR WRITING TO OUTPUT FILES
*---- TINJ      CUMPR1    CUMHI1    WRHPV    WRPRF    RSTC
      435       25        25        20       25       100
CC
CC THE INI. TIME STEP,CONC. TOLERANCE,MAX.,MIN. time steps
*---- DT
      0.00001  0.001 0.2  0.02
CC
CC FLAG FOR INDICATING BOUNDARY CHANGE
*---- IBMOD
      0
CC
CC IRO, ITIME, NEW FLAGS FOR ALL THE WELLS
*---- IRO    ITIME    IFLAG
      1      0        1     2     2     2     2
CC
CC NUMBER OF WELLS CHANGES IN LOCATION OR SKIN OR PWF
*---- NWEL1
      0
CC
```

```
CC NUMBER OF WELLS WITH RATE CHANGES, ID
*---- NWEL2    ID
      1       1
CC
CC ID,INJ. RATE AND INJ. COMP. FOR RATE CONS. WELLS FOR EACH PHASE
(L=1,3)
*----  ID   QI(M,L)   C(M,KC,L)
      1 17643.776   1   0   0   0 0.0553 0.001 0   0   0 1.0   0
      1   0         0   0   0   0   0      0    0   0   0   0   0
      1   0         0   0   0   0   0      0    0   0   0   0   0
CC
CC CUM. INJ. TIME , AND INTERVALS (PV) FOR WRITING TO OUTPUT FILES
*---- TINJ    CUMPR1    CUMHI1    WRHPV    WRPRF    RSTC
      600      25        25        20       25      100
CC
CC THE INI. TIME STEP,CONC. TOLERANCE,MAX.,MIN. time steps
*----  DT
     0.00001   0.001   0.1   0.01
```

53

References

Choi, S. K., "pH Sensitive Polymer for Novel Conformance Control and Polymer Flooding Application," PhD. dissertation, The University of Texas at Austin, August, 2008.

Flory, P. J., "Principles of Polymer Chemistry," Cornell University Press, Ithaca, New York, 1953.

Kheradmand, H., "Contribution A L'Etude De La Degradation Et La Stabilisation De Polyacrylamides En Solution Aqueuse," These Pour Obtenir Le Grade De Docteur D'Etat Es Sciences Physiques, Universite Louis Pasteur De Strasbourg, Strasbourg, France, 1987.

Koning, E.J.L., Mentzer, E., and Heemskerk, J., "Evaluation of a Pilot Polymer Flood in the Marmul Field, Oman," SPE 18092 presented at the 63rd Annual Technical Conference and Exhibition of the Society of Petroleum Engineers, Houston, TX, October 2-5, 1988.

Kulicke, W.M. and Horl, H.H., "Preparation and characterization of a series of poly(acrylamide-co-acrylates), with a copolymer composition between 0-96.3 mol-% acrylate units with the same degree and distribution of polymerization," *Colloid & Polymer Science* **263:** 530-540, 1985..

Lakatos, I., Lakatos-Szabó, J. and Tóth, J. 1979. "Factors Influencing Pilyacrylamide Adsorption in Porous Media and Their Effect on Flow Behavior," Presented at the Symposium on Surface in Phenomena in EOR, Stockholm, Sweden, August. Pleum Publishing Corp., New York.

Lake, L.W., "Enhanced Oil Recovery," Prentice-Hall, Inc., Englewood Cliff, New Jersey, 1989.

Lange, E. A. and Huh, C.: "A polymer Thermal Decomposition Model and Its Application in Chemical EOR Process Simulation," SPE/DOE 27822 presented at the SPE/DOE 9th Symposium on Improved Oil Recovery, Tulsa, Oklahoma, April 17-20, 1994.

Levitt, D. B., "The Optimal Use of Enhance Oil Recovery Polymers under Hostile Conditions," PhD. dissertation, The University of Texas at Austin, May, 2009.

Levitt, D.B., Pope, G.A., and Jouenne, S., "Chemical Degradation of Polyacrylamide Polymers Under Alkaline Conditions," Paper SPE 129879 presented at the Improved Oil Recovery Symposium, Tulsa, OK, April 24-28, 2010.

Mohammadi, H., "Mechanistic Modeling, Design, and Optimization of Alkaline/Surfactant/Polymer Flooding," PhD. Dissertation, The University of Texas at Austin, 2008.

Moradi-Araghi, A. and Doe, P.H., "Hydrolysis and Precipitation of Polyacrylamides in Hard Brines at Elevated Temperatures," *SPERE* 189-198, 1987.

Muller, G., "Thermal Stability of High-molecular-weight Polyacrylamide Aqueous Solutions," Polymer Bulletin 5: 31-37, 1981.

Putz, A.G., Lecourtier, J.M., and Bruckert, L., "Interpretation of High Recovery Obtained in a New Polymer Flood in the Chateaurenard Field," SPE 18093 presented at the 63rd Annual Technical Conference and Exhibition of the Society of Petroleum Engineers, Houston, TX, October 2-5, 1988.

Ryles, R.G., "Chemical Stability Limits of Water-Soluble Polymers Used in Oil Recovery Processes. Paper SPE 13585 presented at the SPE Symposium on Oilfield and Geothermal Chemistry, Phoenix, April 9-11, 1988.

Seright, R.S. and Mozley, P.S., "Stability of Partially Hydrolyzed Polyacrylamides at Elevated Temperatures in the Absence of Divalent Cations," Paper SPE 121460 presented at the international Symposium on Oilfield Chemistry, Woodlands, TX 20-22 April, 2009.

Sorbie K. S., "Polymer-Improved Oil Recovery," Blackie and Son Ltd, Glasgow, 1991.

UTCHEM Volume II: Technical Documentation for UTCHEM-9.0, Center for Petroleum and Geosystems Engineering, University of Texas at Austin, 2000. http://www.cpge.utexas.edu/utchem/UTCHEM_Tech_Doc.pdf

Wang, D., Xia, H., Liu, Z., and Yang, Q. 2001. Study of the Mechanism of Polymer Solution with Visco-Elastic Behavior Increasing Microscopic Oil Displacement Efficiency and the Forming of Steady 'Oil Thread' Flow Channel. SPE 68723 presented at SPE Asia Pacific Oil Gas Conference, Jakarta, Indonesia, 17-19 April.

Zaitoun, A. And Potie, B. 1983. Limiting Conditions for the Use of Hydrolyzed Polyacrylamides in Brines Containing Divalent Ions. Paper SPE 11785 presented

at the International Symposium on Oilfield and Geothermal Chemistry, Denver, CO 1-3 June.

Vita

Ahra Lee was born in Dague, South Korea. She entered Seoul National University in Seoul, Korea and received a Bachelor of Science degree in Civil, Urban, and Geosystem Engineering in 2003 and awarded the degree of Masters of Science in Geoenvironmental Engineering from Seoul National University, Korea in 2005. She accomplished a Masters of Science degree in Petroleum Engineering from the University of Texas at Austin in 2010. She was a Graduate Research Assistant at the Center for Petroleum & Geosystems Engineering (CPGE)'s Chemical Enhanced Oil Recovery group between January 2009 and December 2010.

Email address: lee.ahra@gmail.com.

This report was typed by the author.